

UC Berkeley

UC Berkeley Previously Published Works

Title

Ocean-atmosphere dynamics linked to 800–1050 CE drying in mesoamerica

Permalink

<https://escholarship.org/uc/item/71f2s32w>

Authors

Bhattacharya, Tripti

Chiang, John CH

Cheng, Wei

Publication Date

2017-08-01

DOI

10.1016/j.quascirev.2017.06.005

Peer reviewed

Ocean-atmosphere dynamics linked to 800–1050 CE drying in mesoamerica

Author links open overlay panel [TriptiBhattacharya](#) · [John C.H.Chiang](#) · [WeiCheng](#)
Show more

<https://doi.org/10.1016/j.quascirev.2017.06.005> Get rights and content

Highlights

-

Proxy records show coherent interval of drying in Mesoamerica, between 800 – 1050 CE.

-

Mesoamerican drought linked to Atlantic variability in climate model simulations.

-

Regional drought may be linked to the North Atlantic Subtropical High (NASH).

-

Cooler tropical north Atlantic weakens convection over southern central America.

Abstract

Proxy records from the last millennium in Mesoamerica suggest a widespread interval of drought at some point between the 7th and 13th centuries CE. In some records, this time period represents the driest proxy values in the last few millennia. There is currently no clear dynamical explanation for these droughts, nor consensus as to whether they were spatiotemporally coherent over the region. We perform several analyses to develop a novel hypothesis to explain these droughts that is consistent with our knowledge of the dynamics of the climate system. We use Bayesian age modeling techniques and a synthesis of regional proxy records to suggest that there is robust evidence of drying between 800 and 1050 CE, with the sites showing dry conditions clustered in southern central America. By studying control simulations of two [general circulation models](#) (GCMs), we suggest that this pattern may be diagnostic of hydroclimate changes associated with multidecadal variability in the Atlantic Basin. Models and instrumental data suggest that cooling of tropical Atlantic [SSTs](#) and strengthening of the North Atlantic Subtropical High drives a pattern of multidecadal drought with negative rainfall anomalies in southern central America and positive

anomalies in northern Mexico. This process could have resulted in the droughts observed in the proxy record. Our work offers a novel hypothesis about the dynamics of multidecadal drought in Mesoamerica, and builds on previous efforts to synthesize proxy records from the region.

- [**Previous article**](#)
- [**Next article**](#)

Keywords

Central America

Paleoclimatology

Proxy-model synthesis

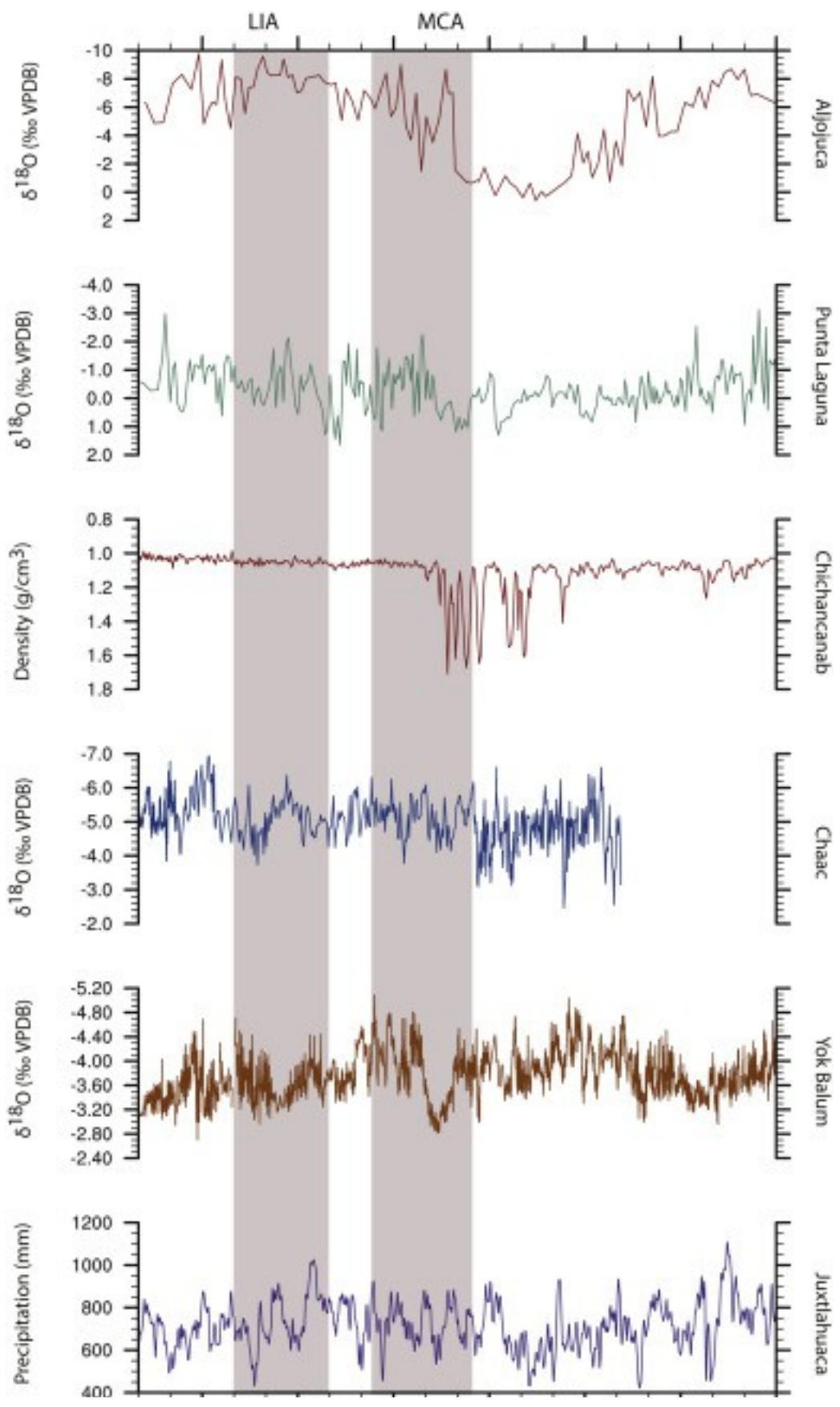
Climate dynamics

Holocene

Drought

1. Introduction

In recent years, much research has focused on clarifying the pattern of late [Holocene](#) drought in Mesoamerica. This has largely been motivated by an interest in the cultural implications of drought for pre-Columbian societies ([Curtis et al., 1996](#), [Webster et al., 2007](#), [Akers et al., 2016](#), [Medina-Elizalde et al., 2010](#), [Lachniet et al., 2012](#), [Kennett et al., 2012](#), [Bhattacharya et al., 2015](#)). Records of past drought come from lacustrine proxy records, which are sensitive to precipitation minus evaporation (P-E) ([Fig. 1](#), top three panels), or [speleothem](#) records that are largely controlled by the amount of annual precipitation ([Fig. 1](#), bottom three panels). A robust feature of many of these lake and speleothem proxy records is a dry interval pre-dating or during the Medieval Climate Anomaly (MCA; 950–1250 CE) ([Fig. 1](#)) ([Mann et al., 2009](#)). In many cases this interval is one of the driest in the last millennium or several millennia, although several records also indicate drying during the [Little Ice Age](#) (LIA; 1400–1700 CE) ([Fig. 1](#)).



1. [Download high-res image \(662KB\)](#)
2. [Download full-size image](#)

Fig. 1. Selected Mesoamerican proxy records to highlight debates about drought timing before and during MCA and LIA. Site names are on the right side of each plot, see text for references. Gray bars identify the MCA and the LIA, as defined by [Mann et al. \(2009\)](#). On each plot, 'down' indicates drier conditions. See [Supplemental Table A.1](#) for a brief review of each proxy type.

Many authors argue that these proxy records highlight a region-wide interval of drought, and invoke large-scale [climate dynamics](#) as a cause of the drying. Some have argued that these droughts represent a southward migration of the [Intertropical Convergence Zone](#) (ITCZ), or reductions in the frequency of [tropical storms](#) ([Medina-Elizalde and Rohling, 2012](#), [Haug et al., 2003](#)). However, these hypotheses do not elucidate the processes that would shift the [ITCZ](#) or change storm frequencies. Modeling studies suggest that anthropogenic [deforestation](#) amplified pre-Columbian drought ([Oglesby et al., 2010](#), [Cook et al., 2012](#)), which is not inconsistent with a large-scale dynamical driver of drought. More recently, [Lachniet et al. \(2017\)](#) suggested that a proxy record in western Mexico is influenced by changes in the North Atlantic as well as the eastern equatorial Pacific. However, this work focuses on a single proxy site and uncertainty remains as to whether there is robust proxy evidence for a spatially coherent time period of regional drying, or whether the proxies record different, non-overlapping dry intervals.

In this paper, we explore the available proxy evidence for droughts in the last 2000 years in Mesoamerica, and undertake several analyses to identify their timing and dynamical origin. We first evaluate whether the proxy evidence for a regionally coherent interval of drying at any point before or during the MCA. given that many proxy records are dated using radiometric techniques with significant age uncertainty, establishing the timing of dry intervals across multiple records is not straightforward. We then use instrumental data and [general circulation model](#) (GCM) simulations to explore the dynamics that result in long-term drought in Mesoamerica. We do not explicitly simulate particular drought events. Rather, our approach is to use long, unforced [GCM](#) simulations, or control simulations, to study the changes to the [atmosphere-ocean system](#) that drive hydroclimate in Mesoamerica. This approach can clarify the processes and mechanisms underlying local hydroclimate variability, helping us generate hypotheses about the causes of past changes. Even if external forcing is responsible for a particular event, our approach using control simulations is valuable because the signal of external forcing must be communicated to local climate

through changes in the ocean-atmosphere system. An additional advantage of this approach over simply analyzing the correlation between Mesoamerican rainfall and known climate modes is that our approach can help pinpoint the specific dynamical mechanisms that connect [remote regions](#) to Mesoamerica. As a result, it can account for non-stationarity in the teleconnections between Mesoamerican climate and large-scale climate modes as well as non-stationarity in these modes themselves.

1.1. Background and outline

Mesoamerica, a region on the [isthmus](#) joining North and South America, has a strongly seasonal climate. Convective activity peaks from May through October, although many regions feature a mid-summer minimum in precipitation known as the canícula ([Giannini et al., 2000](#)). Dry conditions during boreal winter are associated with the expansion of the North Atlantic Subtropical High ([Giannini et al., 2000](#)). Warm tropical North Atlantic [SSTs](#), southeasterly moisture transport into the Intra-Americas Seas, and the propagation of easterly waves across the Atlantic favor summertime convective activity ([Mestas-Nuñez et al., 2007](#)). Despite this climatic diversity, large-scale climatic modes can produce coherent rainfall anomalies across the region: interannual variability has been strongly linked to the [El Niño Southern-Oscillation](#) (ENSO) and the NAO ([Giannini et al., 2000](#), [Magaña et al., 2003](#), [Mestas-Nuñez et al., 2007](#), [Méndez and Magaña, 2010](#)). Interannual variability has also been linked to changes in tropical North Atlantic [sea surface temperatures](#) (SSTs) ([Wang et al., 2008](#), [Xie and Carton, 2004](#)). This paper focuses on two major research questions: is there coherent evidence for drying across Mesoamerica at some point between 600 and 1200 CE? Second, what mechanisms are responsible for past dry intervals? To answer these questions, we first review the proxy records from the region to establish the precise interval during which they indicate anomalously dry conditions. Next, we explore the relationship between Mesoamerican climate and major climate modes using instrumental data. The purpose of this analysis is to facilitate a review of what is known about climate variability in this region in the published literature. Finally, the limited length of the observational record and uneven station coverage hinders our ability to quantify the magnitude and precise spatial pattern of past droughts. We therefore use coupled atmosphere-ocean general circulation models (GCMs) to identify the dominant modes of low-frequency climate variability influencing Mesoamerica. We conclude by proposing hypotheses about the dynamical drivers of long-term droughts in Mesoamerica.

2. Data sources and methods

2.1. Analysis of Mesoamerican proxy records

Our first goal is to identify periods during the last two millennia when multiple proxy records show evidence for drying. We identified key records via literature search, and where possible, we obtained the raw lacustrine and [speleothem](#) proxy data from available online databases (i.e. NOAA/NCDC) or original papers' supplemental text ([Figure A.11](#)). Our analysis had two components: first, we compiled records that show evidence of a dry interval at some point between 600 and 1200 CE to identify whether there is reasonable evidence that intervals at disparate locations overlap in time. After identifying an interval of widespread drought, we mapped whether proxy sites showed dry, wet, or neutral conditions during that particular interval.

We restricted our analysis to proxy records that cover at least the last 1500–2000 years, have multidecadal to at least sub-centennial sampling resolution, and 5 or more radiocarbon or other dates in the last 2000-year interval. These criteria allow us to ensure that records have sufficient [temporal resolution](#) and chronological precision to capture multidecadal-to centennial-scale dry intervals.

The proxy records included in this synthesis also feature an independent hydroclimate proxy, which allows us to disentangle climatic and anthropogenic activity (i.e. pollen or [charcoal](#), which are often influenced by human activities, is excluded). The majority of sites record changes in total rainfall or precipitation minus evaporation (P-E), with the exception of [van Hengstum et al. \(2016\)](#) and [Woodruff et al. \(2008\)](#), where [coastal sediment](#) sequences provide evidence of [hurricane](#) frequencies. The full suite of sites is included in [Figure A.11](#) and [Table Appendix A](#).

2.2. Lacustrine sites

Identifying the timing of drought events in lake records is largely difficult because of their time-uncertain radiocarbon-based chronologies. To overcome some of these difficulties, we included lacustrine sites that had both the raw proxy data and radiocarbon dates available (i.e. the sites included in [Fig. 1](#)) in a [Bayesian analysis](#) of drought timing. This analysis was limited to three sites: Chichancanab, studied by [Hodell et al., 2005a](#), [Hodell et al., 1995](#); Punta Laguna, studied by [Curtis et al. \(1996\)](#); and Aljojuca, studied by [Bhattacharya et al. \(2015\)](#). All three sites show significant drying in the time period prior to and during parts of the MCA.

For the three available lake records, we used the Bayesian age modeling program BACON to quantify age uncertainty associated with each proxy record ([Blaauw et al., 2011](#)). The program uses [Markov Chain Monte Carlo](#) simulations to propagate the age uncertainty associated with each radiocarbon date through the entire age model. We

used all available radiocarbon dates for each site, barring significant age reversals (see [Supplemental Figure A.12](#)). To identify the timing of dry intervals, we transformed proxy values so that lower values indicated dry conditions (i.e. multiplying measurements by -1) and identified the lowest 17th percentile of the data as indicative of significant [aridity](#). This would be equivalent to one standard deviation from the mean if the proxy data were normally distributed. We then used the BACON function 'Events' to quantify the probability of arid conditions at any calendar age covered by the record ([Blaauw et al., 2011](#)). To calculate the composite probability of drought across all proxy sites in a given time interval, we took the product of individual sites' drought probability. As an assessment of statistical significance, we replaced each lake record with red noise generated with an autoregressive process (AR1), and performed the Bayesian analysis with this simulated data to identify the probability of obtaining drought across all three sites by chance alone. When the probability of drought across the actual proxy records exceeds this threshold, we suggest that this is evidence of a significant interval of drought.

We also qualitatively compare the estimates of the timing of aridity in other radiocarbon-based lake and marine records by plotting the interval when each of these sites shows dry conditions. This offers a rough estimate of the timing of dry conditions across the region, despite age uncertainty influencing each of these sites.

2.3. Speleothem records

A distinct feature of many speleothem records is the relatively precise chronology offered by U-Th dating or layer-counting, which is more precise than radiocarbon and often results in absolutely-dated records ([Douglas et al., 2016a](#)). Similarly, the chronology for the Cariaco Basin is anchored by [varve](#) counts for the early [Holocene](#), which decreases the age uncertainty in this proxy record ([Haug et al., 2003](#)).

Exploratory analyses suggested that including these records in our Bayesian framework yielded discrete jumps in drought probabilities: inferred drought probability was close to 100% likely in decades the authors identified as representing drought, while close to 0% at other intervals due to the lower age uncertainty associated with the chronologies.

This is distinct from radiocarbon-based chronologies, which yield drought probabilities that are more evenly 'smeared'-out over a given time interval. As a result, we quantify drought probabilities at precisely-dated sites by plotting the interval when each of these sites shows dry conditions using a horizontal blue bar, since Bayesian analysis yields nearly identical results for the centennial-scale patterns we identify in this paper.

2.4. Other records

We do not consider [tree ring](#) records in this analysis, because existing tree rings records from Mesoamerica generally reflect early spring rainfall, and may reflect a distinct climatic signal from that recorded by speleothem and lake records ([Stahle et al., 2012](#)). We do, however, consider the evidence available from tree ring records when discussing teleconnections between Mesoamerican climate and the large-scale climate system.

2.5. Mesoamerican hydroclimate variability in the instrumental record

In this section, we outline what is known about variability in Mesoamerican climate from studies of the instrumental record. To guide our analyses, we focus on studies of major modes of climate variability (e.g. [ENSO](#), NAO, etc) and their impact on the region. However, our goal in this section is not to suggest that these modes were directly responsible for past hydroclimate changes in Mesoamerica. Rather our goal is to identify the *dynamical mechanisms* by which these modes influence the climate of Mesoamerica. By identifying these mechanisms, we can generate precise hypotheses about the physical processes that may have been key in driving past droughts. To guide our analyses, we have plotted the correlation of key climatic modes with annually-averaged instrumental rainfall data, taken from the 0.5° Global Precipitation Climatology Centre's dataset ([Schneider et al., 2014b](#)). To ensure adequate spatial coverage of rainfall data, correlations are only plotted between 1930 and 2010. We focus on several climatic modes:

-

The [El Niño Southern-Oscillation](#) (ENSO) system refers to changes in the zonal gradient of [sea surface temperatures](#) (SST) in the equatorial Pacific, and consequent changes to the Pacific Walker Circulation. [El Niño](#) events represent anomalous warm conditions in the eastern equatorial Pacific (EEP), while [La Niña](#) events represent anomalously cool conditions in the EEP. To capture variability in this system, we calculated interannual variability in the DJF Nino 3.4 index, which captures changes in the zonal gradient of [SST](#) averaged over a region spanning 5° S– 5° N and 170–120° W ([Trenberth, 1997](#)). We plot two separate correlations with the Nino 3.4 index: to capture Mesoamerican hydroclimate during the developing phase of ENSO events, we plot the correlation of rainfall in the year prior to the DJF Nino 3.4 index (leading correlation, year 0). To capture the delayed response of hydroclimate to a peak

ENSO event, we also plot the correlation of rainfall in the year after the DJF Nino 3.4 index (lagging correlation, year +1).

- The North Atlantic Oscillation, or NAO, is a dominant driver of climate variability over the Atlantic Basin. In its positive phase, it represents an enhancement of the [sea level pressure](#) (SLP) gradient between the Icelandic Low and the North Atlantic Subtropical High (NASH) ([Hurrell and Deser, 2010](#)). In its negative phase, it represents a weakening of this gradient. We use the JFM NAO index for correlation with our rainfall data.

- The Atlantic Multidecadal Oscillation (AMO) index captures basin-wide changes in North Atlantic SSTs, and has been linked to hydroclimate changes across the Atlantic Basin, and may have significant interdecadal variability. We use the unfiltered AMO index as described by [Enfield et al. \(2001\)](#) to illustrate the correlation between this mode and Mesoamerican rainfall.

- While we do not explicitly perform a correlation analysis between the Pacific Decadal Oscillation, a multidecadal oscillation in the Pacific Basin (see [Mantua et al. \(1997\)](#)), we review literature describing its potential impact on Mesoamerican rainfall.

Our goal with our correlation analysis is to motivate our literature review by pointing out the overall sign of the relationship between each mode and Mesoamerican rainfall. We do not perform significance tests since this is simply an exploratory analysis.

2.6. Analysis of low-frequency droughts in GCM simulations

We next consider the dynamical processes that contribute to long-term, multidecadal to centennial scale dry periods as observed in proxy records from the last two millennia across Mesoamerica. Because of temporal limitations of the instrumental record, we rely on [GCM](#) control simulations to analyze the processes that produce long-term droughts. Control simulations represent long [climate model](#) experiments run without changing external forcing, and they simulate the natural variability of the climate system. Years in the control simulation do not correspond to calendar years. Instead, control simulations offer an indirect method for exploring mechanisms underlying [paleoclimate](#) change. These simulations can show the preferred configurations of the larger [atmosphere-ocean system](#) associated with regional [climate changes](#), and test the correlations between climatic modes or large-scale features and

local conditions. This is distinct from explicitly prescribing changes to a particular mechanism in a ‘forced’ model experiment. Control simulation-based analyses are critical, because even if external forcing plays a role in particular regional droughts, it must be communicated to particular regions via changes in the large-scale atmosphere ocean system. Our goal is to clarify the large-scale changes associated with low-frequency Mesoamerican droughts.

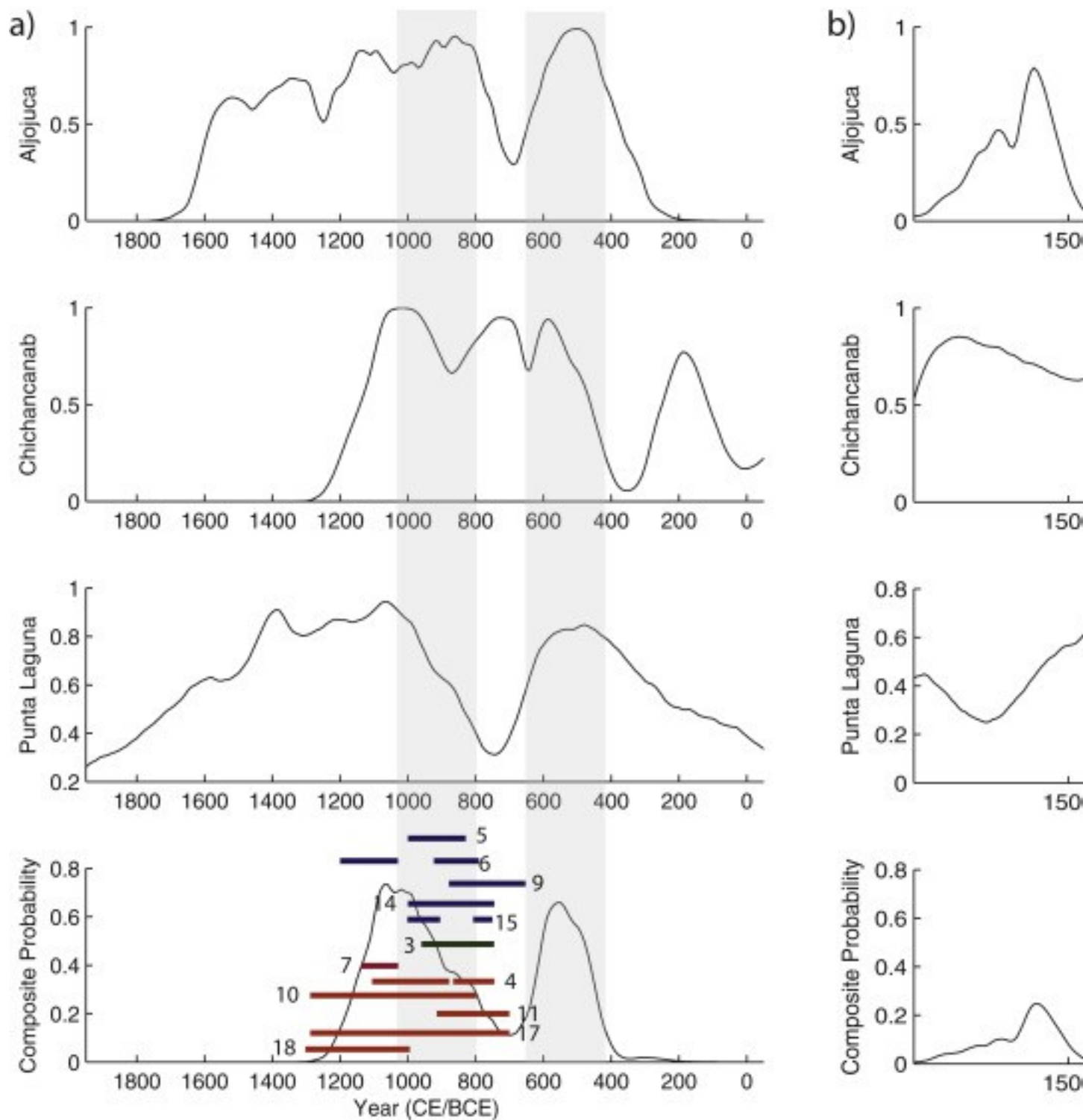
We used fields of precipitation, evaporation, SST, SLP, winds, and humidity from a 1200-year pre-industrial control simulation of the Hadley Centre's HadCM3 model ([Gordon et al., 2000](#)), and a 1300-year pre-industrial control simulation of the Community Climate System Model (CCSM4) ([Gent et al., 2011](#)) in the [Coupled Model Intercomparison Project 5](#) (CMIP5) archive. We checked both models to see that they produce a realistic modern [climatology](#) over Mesoamerica.

In order to analyze regional droughts across in Mesoamerica, we first define a timeseries that captures broad, regional-scale features of hydroclimate variability in Mesoamerica. This is challenging, because the region features a variety of climatic and ecological regimes. To summarize regional variability in both model simulations, we first applied a low-pass Butterworth filter to rainfall data over the land area of Mesoamerica in order to remove sub-decadal variability (<10years) and emphasize multidecadal, low-frequency changes. We then decomposed this spatiotemporal dataset into fundamental modes of variability, or [empirical orthogonal functions](#) (EOFs). [EOF analysis](#) is equivalent to [principal component analysis](#), and summarizes the variability in a spatiotemporal dataset by producing a series of orthogonal spatial modes that are linear combinations of the original data. A map of the ‘weights’ applied to the original data, or the regression of the PC onto local rainfall, helps identify the spatial pattern represented by each EOF timeseries, with grid cells with the same sign co-varying together. Analysis of the associated time series provides information on changes in that mode over time. We used the time series associated with the first EOF of Mesoamerican rainfall in both CCSM4 and HadCM3 to identify multidecadal droughts. These droughts are defined by at least 20-year periods of below-average scores of EOF1, where the end of a drought is signaled by five or more contiguous positive EOF timeseries values. We choose these long drought intervals for analysis because they likely represent the type of low-frequency variability recorded by proxies. We analyze the anomalies of SST, specific humidity, and winds associated with these dry intervals in order to elucidate their underlying dynamics.

3. Results

3.1. Analysis of proxy records

Synthesis of Mesoamerican proxy records suggests that there are significant time intervals in the past when records do show coherent evidence of drying. The analysis suggests that 800–1050 CE is a time period of coherent drying across the region, extending across Mesoamerica. [Fig. 2a](#) shows the results of our [Bayesian analysis](#) of the timing of dry intervals, performed with the three lacustrine records where all data was available. [Fig. 2b](#) shows the same lacustrine records where the proxy time series have been replaced with red noise to simulate dry intervals that may occur simply as a result of chance. The analysis performed with red noise data suggests that the composite probability of dry conditions across all lake sites never exceeds 0.3 simply as a result of chance ([Fig. 2b](#)). The analysis with the actual lacustrine proxies shows two significant intervals where probability of composite drought across all three lacustrine sites is greater than 0.3: a period between 400 and 600 CE, and 800 to 1200 CE. Including the estimates of drought timing from other sites in the literature narrows the latter interval to 800 to 1050 CE ([Fig. 2a](#)).



1. [Download high-res image \(562KB\)](#)
2. [Download full-size image](#)

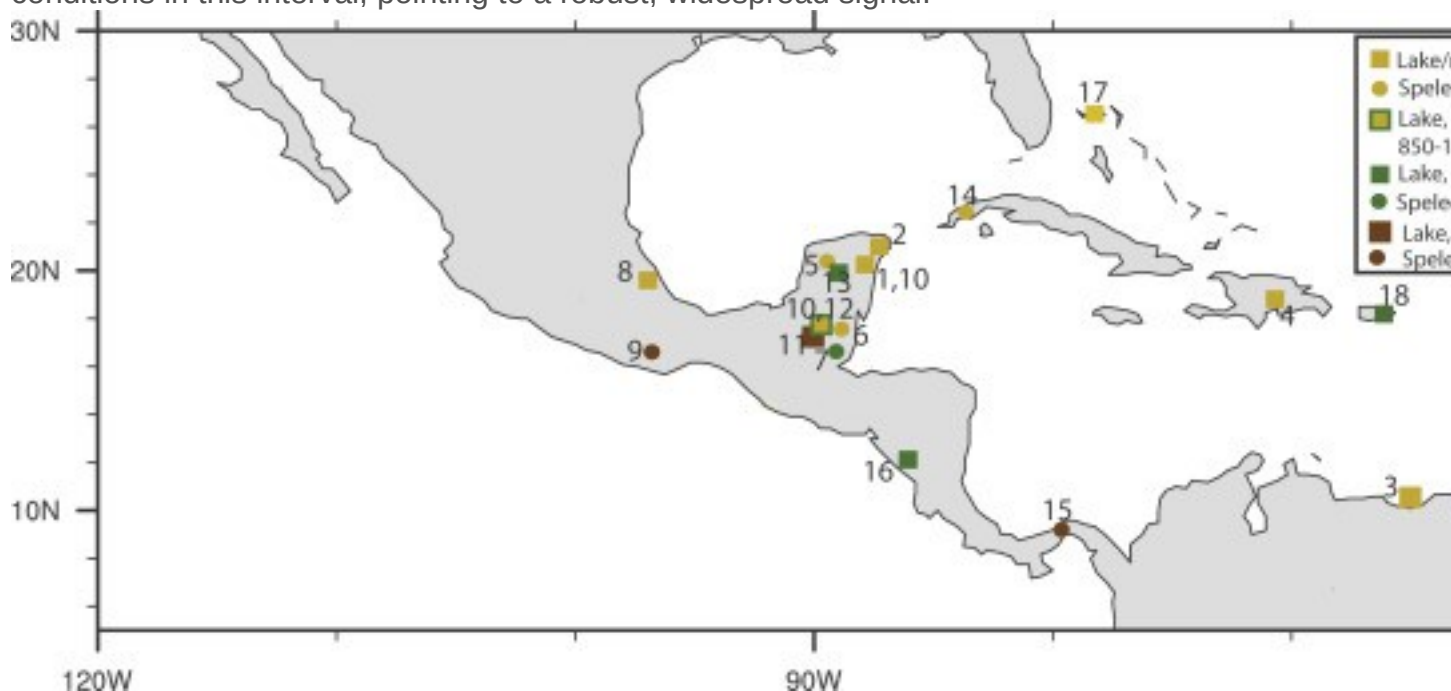
Fig. 2. Results of age [uncertainty analysis](#) for proxy sites: a) displays drought probabilities in given time intervals for the actual proxy data, with gray bars indicating

time periods of significant peaks in composite probability. Age models provided in [Supplemental Figure A.12](#). Estimates of drought timing for sites that do include a drought interval between 600 and 1300 CE are included for key [speleothem](#) (blue), marine (green), and lacustrine (red) sites in horizontal bars.

See [Figure A.11](#) and [Table Appendix A](#) for the site numbers. In the case of the Macal Chasm, estimates of drought timing follow the more recent paper by [Akers et al. \(2016\)](#). b) indicates the results from simulated, random proxy data showing that the probability of drought across all three sites never exceeds 0.3 by chance alone. See section [2.2](#). (For interpretation of the references to colour in this figure legend, the reader is referred to the web version of this article.)

To highlight the robustness of this pattern, we plot whether each proxy site shows dry, neutral, or wet conditions between 800 and 1050 CE in [Fig. 3](#). [Fig. 3](#) shows that the majority of proxy sites suggest dry conditions between 800 and 1050 CE. Sites showing dry conditions tend to be below 20° N, with a few exceptions. [Stansell et al. \(2013\)](#) produced a record from Laguna El Gancho in Nicaragua that does not show anomalous wet conditions. Both the [speleothem](#) record from Chilibrillo Cave in Panama, and the Juxtlahuaca speleothem from the Sierra Madre del Sur in Mexico only show dry conditions for part of the interval from 800 to 1050 CE ([Lachniet et al., 2004](#), [Lachniet et al., 2012](#), [Lachniet et al., 2017](#)). El Gancho and Juxtlahuaca are closer to the west coast of Mexico and may reflect different [climatic processes](#) than the other records included here, which are closer to the Atlantic coast. However, on the Yucatan Peninsula, the Yok Balum speleothem suggests a dry interval between 1020 and 1100 CE, postdating the peak dry interval identified here ([Kennett et al., 2012](#)). The site does, however, show more modest drying at 800 CE and may be missing the earlier portion of the drought due to slow growth. Laguna X'Caamal in the Northern Yucatan does not show dry conditions ([Hodell et al., 2005b](#)), and a record from Guatemala's Peten suggests dry conditions earlier, between 680 and 910 CE ([Wahl et al., 2013](#)). The latter two records' estimates of drought timing, however, may be uncertain because of the radiocarbon-based chronology. A [lagoon](#) sediment record from Puerto Rico does not suggest any decrease in tropical storm/hurricane frequencies in this interval ([Woodruff et al., 2008](#)), but a record from the Bahamas shows evidence of suppressed tropical storms ([van Hengstum et al., 2016](#)). In addition, while the 2002 study of Lake Salpeten by [Rosenmeier et al. \(2002\)](#) does not indicate dry conditions, a more recent leaf wax [stable isotope](#) study by [Douglas et al. \(2015\)](#) does show anomalously dry conditions. Despite some exceptions, [Fig. 3](#) clearly shows that 10 of 18 sites show

robust dry conditions between 800 and 1050 CE, and 13 of 18 sites at least partially dry conditions in this interval, pointing to a robust, widespread signal.



1. [Download high-res image \(241KB\)](#)
2. [Download full-size image](#)

Fig. 3. As in Fig. 2, but showing which sites show dry, neutral, or mixed conditions between 800 and 1050 CE. For Lake Salpeten, [Rosenmeier et al. \(2002\)](#) showed neutral conditions, while [Douglas et al. \(2015\)](#) showed evidence of drying using a different proxy. Sites indicated as ‘partially dry’ ([Wahl et al., 2013](#), [Stansell et al., 2013](#), [Lachniet et al., 2004](#)), show dry conditions during multidecadal or centennial periods between 800 and 1050 CE, but not for the majority of the period. See text for more details.

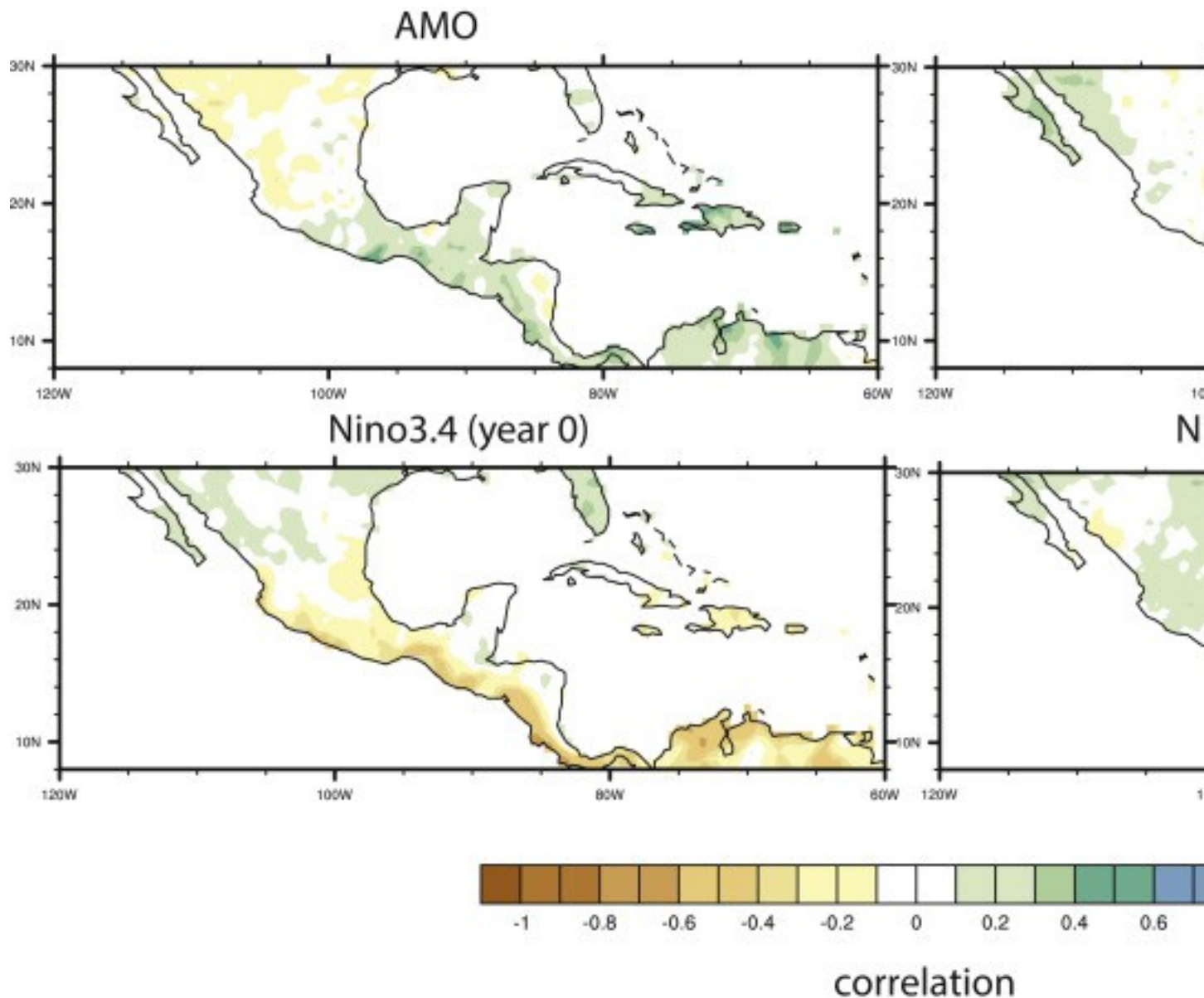
One assumption implicit in our analysis is that lakes and speleothems may reflect similar climatic processes. [Lake level](#) records are sensitive to the ratio of precipitation minus evaporation (P-E). In contrast, speleothem records from Central America are generally interpreted in terms of the ‘amount effect’ with [isotope ratios](#) covarying with the amount of annual precipitation ([Risi et al., 2008](#)). [Douglas et al. \(2016a\)](#) suggest that evaporation and rainfall may show a strong negative correlation, with periods of low rainfall resulting in higher [insolation](#), driving higher [evaporation rates](#). If this is the case, evaporation may act to amplify the [climate signal](#) caused by rainfall, with higher evaporation further drying the land surface in times of reduced rainfall. Reanalysis data that incorporates the instrumental record confirms this idea, by showing a strong negative correlation of evaporation with annual precipitation over land areas ([Uppala](#)

[et al., 2005](#); [Supplemental Figure A.13](#)). The [covariance](#) of precipitation and evaporation over land areas suggests it is reasonable to assume that speleothem records, which in general track total precipitation, and lake records, which track P-E, may ultimately record similar climatic signals. Biases that may complicate the ability of individual sites to record [climate changes](#) are discussed in section [4.1](#).

In sum, [Fig. 2](#), [Fig. 3](#) show a widespread dry signal between 800 and 1050 CE, with a few exceptions. We note that all the proxy sites are clustered in southern central America, consisting of the [Isthmus](#) of Tehantepec to southern Mexico. This could suggest that the drought signal we observe may reflect processes confined to southern central America, but it is difficult to establish this without more well-dated, high resolution proxy records from northern Mexico.

3.2. Mesoamerican hydroclimate variability in the instrumental record

Our exploratory analyses suggest that Atlantic variability results in a dipole of hydroclimate variability in Mesoamerica. We observe a positive correlation between the AMO index and rainfall over southern central America, with an anti-phased correlation in northern Mexico ([Fig. 4](#)). This suggests that on average, warmer conditions across the North Atlantic increase rainfall over Mesoamerica, while the converse is true for cooler conditions. There is support for this idea in the instrumental record and in modeling studies: positive phases of the AMO coincide with an anomalously large Atlantic [Warm Pool](#), creating warm [SST](#) anomalies in the northern tropical Atlantic and the Intra-Americas Sea ([Wang et al., 2008](#)). In modeling studies, warmer SSTs drive increased [boundary layer](#) moisture and convective activity over southern central America. A larger Atlantic Warm Pool may also be associated with increased tropical storms ([Wang et al., 2008](#)). Warm conditions in the tropical Atlantic also decrease the [pressure gradient](#) between the Atlantic and Pacific basins and reduce moisture transport into northern Mexico and the Great Plains ([Wang et al., 2008](#), [Mestas-Nuñez et al., 2007](#)).



1. [Download high-res image \(652KB\)](#)
2. [Download full-size image](#)

Fig. 4. Exploratory correlation of GPCC rainfall data over Mesoamerica with key climatic modes between 1930 and 2010. See text for details of calculations.

Our exploratory analyses suggest that the NAO is negatively correlated with rainfall across much of Mesoamerica, although this correlation is concentrated along the Atlantic coast ([Fig. 4](#)). This coheres with the research of [Giannini et al. \(2000\)](#), who found that the positive phase of the NAO induces stronger [trade winds](#), cooler SSTs, and reduced [atmospheric moisture](#) and precipitation over the Caribbean region. The NAO is known to cause a tripole SST pattern, with cool anomalies in the subtropical and

tropical North Atlantic, warm anomalies in midlatitudes, and cool conditions in subpolar North Atlantic ([Hurrell and Deser, 2010](#)). In the tropical North Atlantic, cooling is a consequence of a wind-SST-evaporation feedback, whereby strengthened trade winds evaporatively cool SSTs ([Deser et al., 2010](#), [Xie and Carton, 2004](#)).

In both the case of the NAO and the AMO, the local dynamical mechanism behind Mesoamerican rainfall changes involves SST variations that drive reductions in boundary layer moisture and convective activity over southern central America. The mechanisms of each mode are distinct: the NAO alters pressure gradients and drives stronger tropical easterlies to reduce SSTs, while the AMO as an index describes basin-wide changes in [surface temperatures](#).

The [ENSO](#) signal in Mesoamerica differs in the developing and decaying phase of the ENSO event: a developing [El Niño](#) event results in anomalous [subsidence](#) and dry conditions in much of Mesoamerica ([Giannini et al., 2000](#)). This is the result of tropical tropospheric warming generated by the anomalous convection in the EEP and consequent southward shifts in the Atlantic [ITCZ](#) ([Chiang and Sobel, 2002](#), [Giannini et al., 2001b](#)). However, following an El Niño event, tropospheric warming induces warming of tropical Atlantic SSTs, and has been shown to result in increased rainfall in the circum-Caribbean region ([Giannini et al., 2000](#)). This effect may be weaker in some regions of [highland](#) Mexico ([Bhattacharya and Chiang, 2014](#)), and can be weakened by the positive phase of the NAO, since a stronger NASH in this phase is associated with stronger trade winds that cool Atlantic SSTs ([Giannini et al., 2001a](#)). ENSO is also known to have an influence on winter rainfall across Mexico and Mesoamerica: El Niño events decrease rainfall over the Isthmus of Tehuantepec, while increasing rainfall over northwestern Mexico ([Magaña et al., 2003](#)). Our correlation analyses illustrate these patterns, showing a negative leading correlation with the DJF Nino3.4 index (year 0) as a result of anomalous subsidence caused by El Niño events. It is interesting to note, however, that the correlation is weaker over the Yucatan Peninsula, and may have opposite signs across regions of the Peninsula. This may explain the differences in the timing of drought between speleothem records from the region noted by ([Douglas et al., 2016b](#)). In contrast, rainfall in the year following the DJF Nino3.4 index illustrates a spatially coherent positive correlation with the index, likely as a result of the delayed warming of SSTs increasing convective activity.

Additional variability in Mesoamerican climate may be tied to the transport of water vapor over the Intra-Americas Sea. The intensity of the Caribbean Low-Level Jet, a maximum in low-level winds in the Caribbean Sea, is linked to variability in northward and westward moisture transport out of the Intra-Americas Sea ([Mestas-Nuñez et al.,](#)

2007, Wang, 2007). Some research suggests that variability in the gradient of SLP between the Atlantic and Pacific Basins enhances the low-level jet: an enhanced gradient drives northward moisture transport into many regions of Mesoamerica. Changes in the CLLJ have been found to track tropical Atlantic SSTs and ENSO phase, while some research suggests that the PDO may also drive changes in moisture transport (Bhattacharya and Chiang, 2014, Méndez and Magaña, 2010).

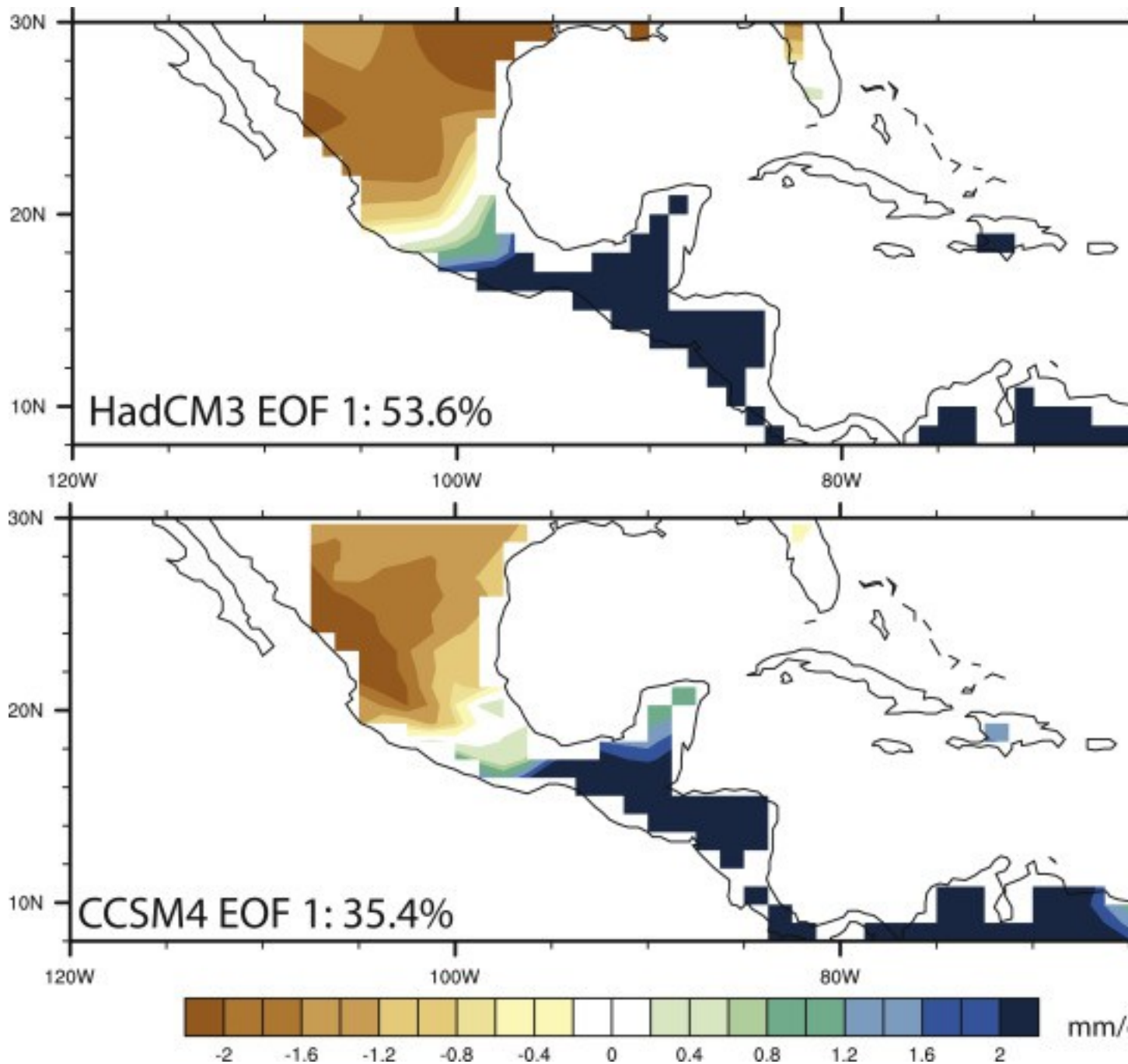
This literature review suggests that several dynamical factors determine hydroclimate variability in Mesoamerica. First, changes in tropical Atlantic SSTs are critical to providing atmospheric moisture to drive local convection. The importance of this influence is illustrated by the teleconnection to the AMO and the NAO. The positive phase of the NAO (through the wind-evaporation-SST feedback), and negative phases of the AMO can act to decrease rainfall by cooling SSTs and reducing the moisture available for convection. In contrast, weakening of the NAO or a positive AMO can drive enhanced convective activity. This influence largely centers on southern central America, with anomalies of opposite sign in northern Mexico as a result of changes in moisture transport driven by wind changes. For instance, variability in the Caribbean Low-Level Jet changes northward and westward moisture transport out of the Intra-Americas Sea, influencing rainfall in northern Mexico. Increases in Atlantic SSTs may actually decrease the strength of the CLLJ by altering the inter-basin gradient of SLP between the Pacific and the Atlantic, reducing [moisture fluxes](#) into northern Mexico. These teleconnections point to the importance of the importance of [latent heat fluxes](#) from the tropical Atlantic and intra-Americas Sea in driving convective activity over southern Mexico and altering moisture fluxes into the eastern Pacific and northern Mexico.

The ENSO teleconnection acts in a different way. The developing phase of an El Niño can increase the threshold for convection by warming the [troposphere](#) and inducing anomalous subsidence. In the decaying phase of an El Niño event, the delayed warming of SSTs may increase rainfall over Mesoamerica. The strength of this latter teleconnection can be influenced by the phase of the NAO. We next contrast these mechanisms with the dynamics responsible for long-term drying in [GCM](#) simulations.

3.3. Low-frequency droughts in control simulations

[EOF analysis](#) reveals that the dominant mode of decadal variability in both models' control simulations represents a dipole of covarying rainfall variability in northern South America, the Isthmus of Tehuantepec, the Yucatan and central Mexico, and anti-phased anomalies in northern Mexico ([Fig. 5](#)). This dipole bears a strong similarity to the pattern

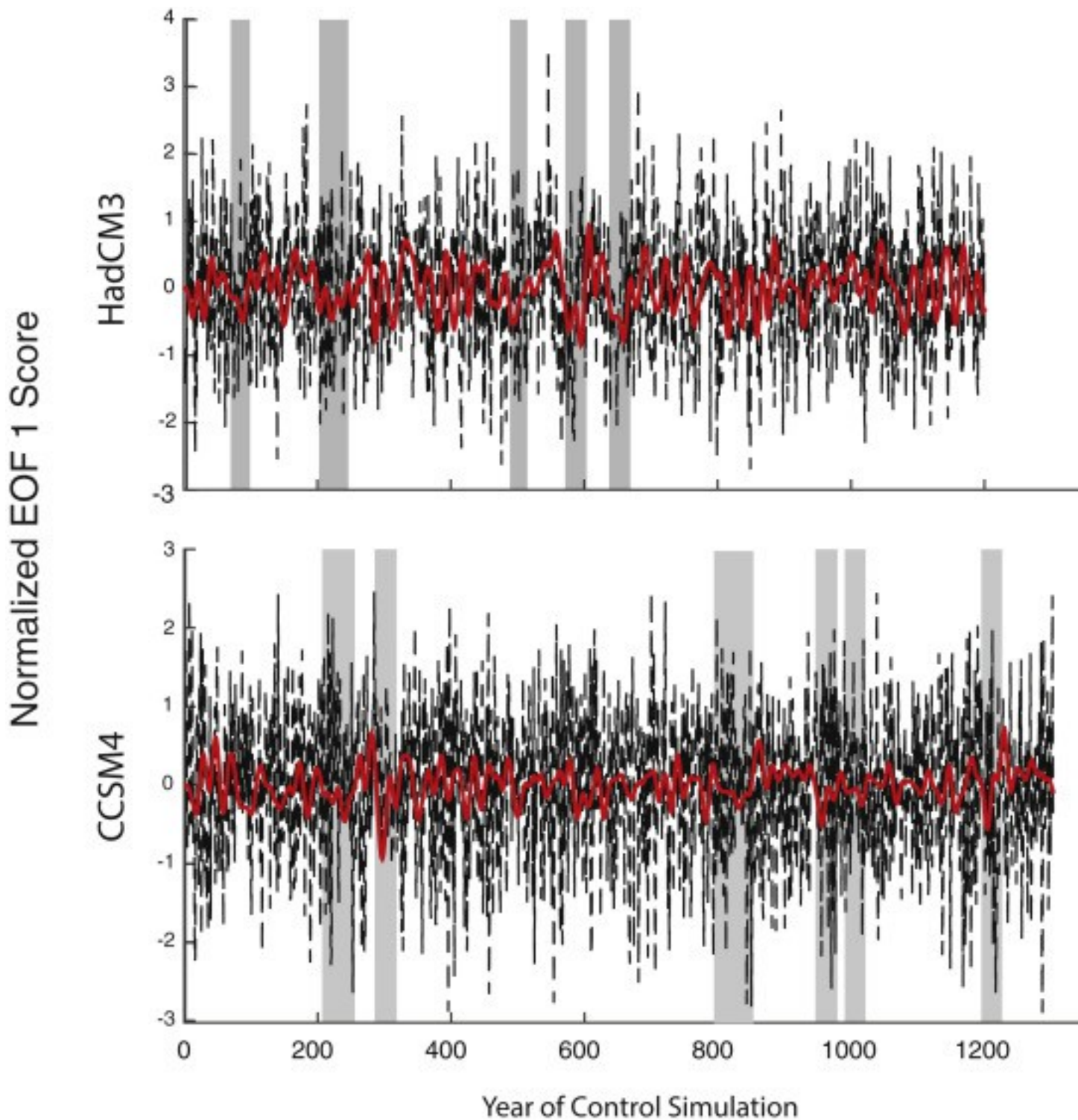
associated with Atlantic variability in the instrumental record. In CCSM4, this pattern represents approximately 35% of the variance in the rainfall field, with the boundary between negative and positive anomalies occurring at approximately 18° N. The model, at a 1° resolution, lacks the resolution to resolve detailed hydroclimate patterns on Caribbean islands. In HadCM3, the pattern is nearly identical, apart from the fact that EOF 1 explains 53.6% of the variance in low-pass filtered rainfall in this model. The HadCM3 control simulation is at a 2° resolution, but for the purposes of this analysis we regridded the data to a 1° resolution. While neither model resolves fine-scale patterns on the Caribbean islands, the EOF1 pattern in both models provides a useful method to summarizing the dominant pattern of rainfall variability over Mesoamerica.



1. [Download high-res image \(476KB\)](#)
2. [Download full-size image](#)

Fig. 5. Spatial pattern of first EOF of low-frequency Mesoamerican rainfall, after masking out ocean areas in CCSM4 and HadCM3 control runs. Models were regridded to 1° resolution. Variance in the rainfall field explained by each EOF displayed on the plot, and units are mm/day of rainfall associated with 1 unit change in PC1.

The low-pass filtered timeseries of the EOF pattern in both models reveal extended periods of dry conditions over Mesoamerica. In CCSM4, PC1 shows six periods of multidecadal drought in southern central America, and in HadCM3, there are five multidecadal dry intervals ([Fig. 6](#)). The [regression analysis](#) shown in [Fig. 5](#) shows that a 1 unit reduction in PC1 is associated with 2 mm/day drying in southern central America in both models, which suggests that the 0.4–0.5 PC1 unit reduction in the long drought intervals from [Fig. 6](#) could be associated with a 20–30% reduction in annual rainfall in many regions.

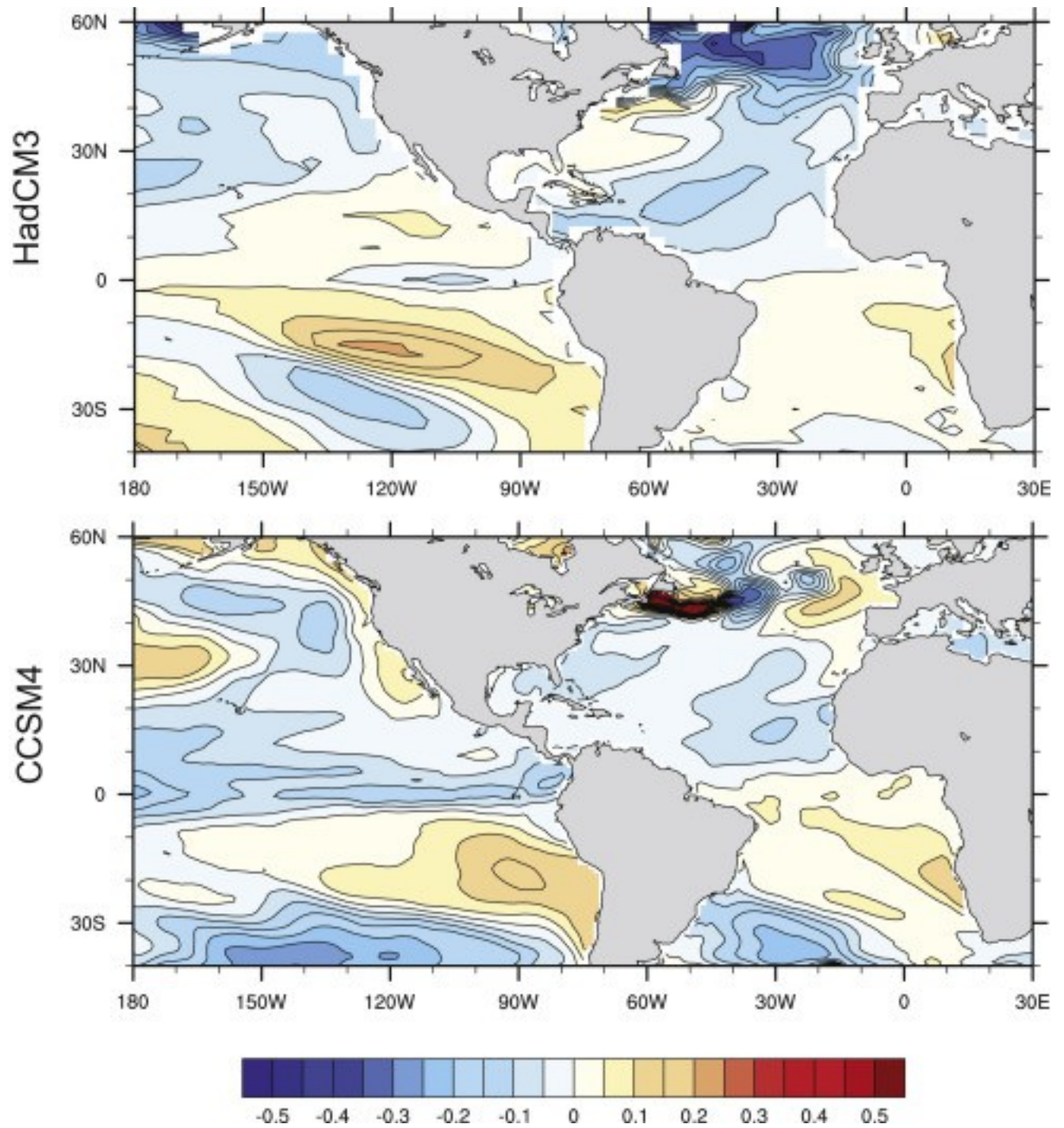


1. [Download high-res image \(998KB\)](#)
2. [Download full-size image](#)

Fig. 6. Raw timeseries of PC1 (time series of EOF1) for CCSM4 and HadCM3 (black line), and multidecadal filtering (red line). Significant drought intervals meeting criteria

outlined in section [2.6](#) are highlighted in vertical gray bars. (For interpretation of the references to colour in this figure legend, the reader is referred to the web version of this article.)

SST composites associated with these dry intervals show a pattern of cooling in the North Atlantic, with the largest SST anomalies occurring at high latitudes, although negative anomalies propagate into the tropical North Atlantic ([Fig. 7](#)). Negative SST anomalies in the tropical North Atlantic are accompanied by slight warming or neutral conditions in the tropical South Atlantic, creating an interhemispheric gradient of SST. Both models also show that drought intervals are associated with increases in equatorial Pacific SSTs, the centre of action for the [El Niño Southern Oscillation](#). However, the SST pattern in the Pacific ocean does not resemble a traditional El Niño, as the SST anomalies are slightly south of the [equator](#) in both models, and do not extend up the coast of north America. Interannual rainfall changes in both models are correlated with ENSO events, but that this correlation decays once we analyze only low-frequency hydroclimate variability (not shown). The congruent results in both HadCM3 and CCSM4 suggest that droughts in Mesoamerica are dynamically related to cooling in the North Atlantic. We next explore the processes that are locally responsible for dry conditions over Mesamerica by analyzing changes in the atmosphere during extended dry intervals.

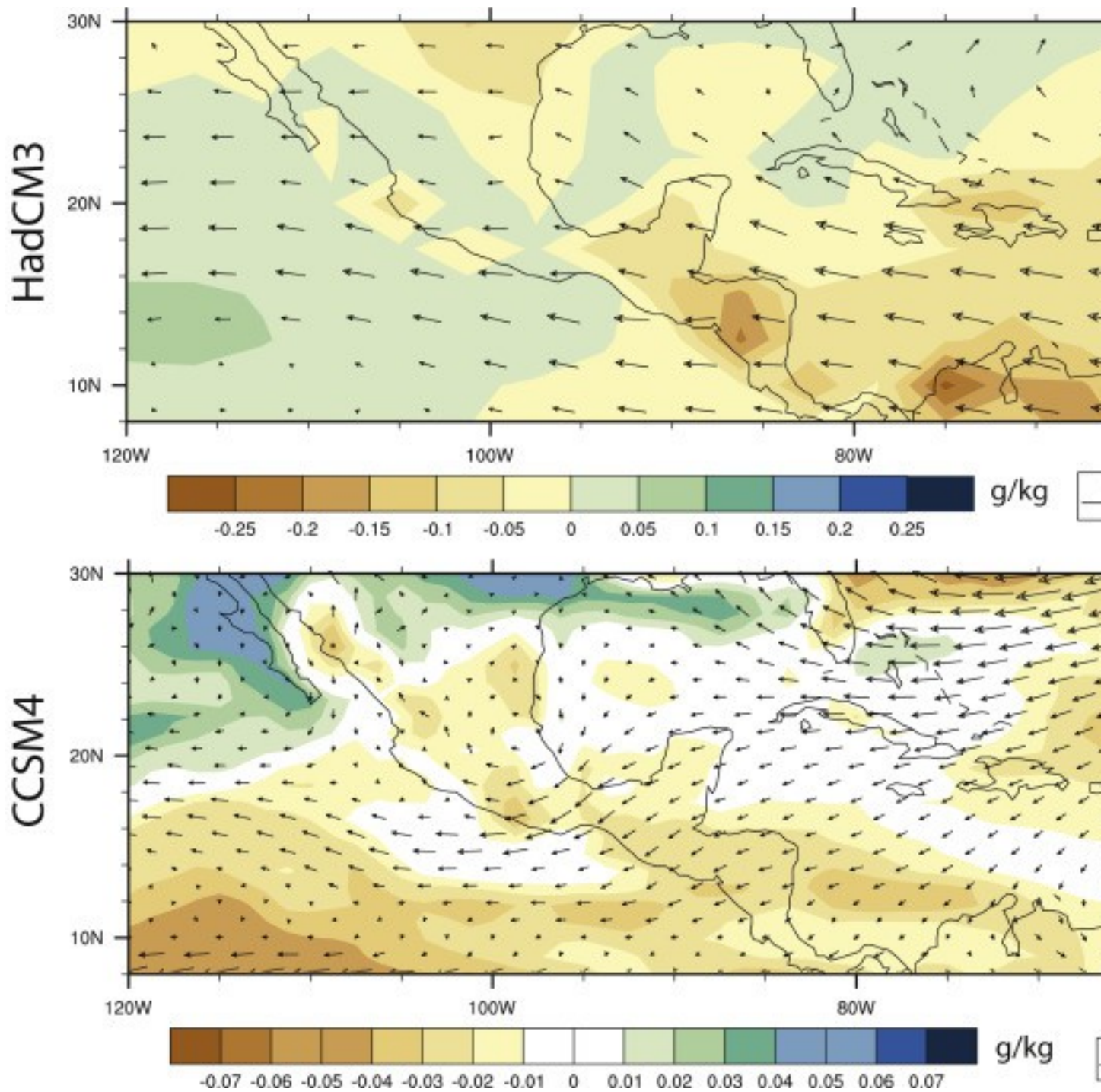


1. [Download high-res image \(883KB\)](#)
2. [Download full-size image](#)

Fig. 7. [SST](#) composites associated with the multidecadal dry periods highlighted in gray bars in [Fig. 6](#).

In [Fig. 8](#), we show the low-level changes in humidity and winds associated with Mesoamerican drought, plotted as composites for the dry intervals in [Fig. 6](#). Both

CCSM4 and HadCM3 control simulations show similar dynamical changes during extended dry intervals over southern central America. In HadCM3, low-level moisture decreases over northern tropical South America and southern central America, most likely in response to the cooling of tropical North Atlantic SSTs (see [Fig. 7](#)). There are also easterly wind anomalies across the Isthmus of Tehuantepec and much of Mesoamerica. Stronger easterly moisture transport on the western boundary of the Intra-Americas Sea has been linked to increased moisture divergence and decreased precipitation over Mesoamerica ([Mestas-Nuñez et al., 2007](#)). This easterly moisture transport also converges moisture over the eastern Pacific ([Fig. 8](#)). The pattern in CCSM4, although different in magnitude than HadCM3, illustrates the same basic pattern as that found in HadCM3. There is strong drying over southern central America, although in contrast to HadCM3, this drying extends into the eastern Pacific. In northern Mexico, at approximately 28° N, we see increased moisture convergence over the land area and especially in the eastern Pacific. These changes are also accompanied by easterly wind anomalies over southern central America ([Fig. 8](#)). As in HadCM3, these easterly anomalies likely contribute to moisture divergence over the Intra-Americas Sea and southern central America.



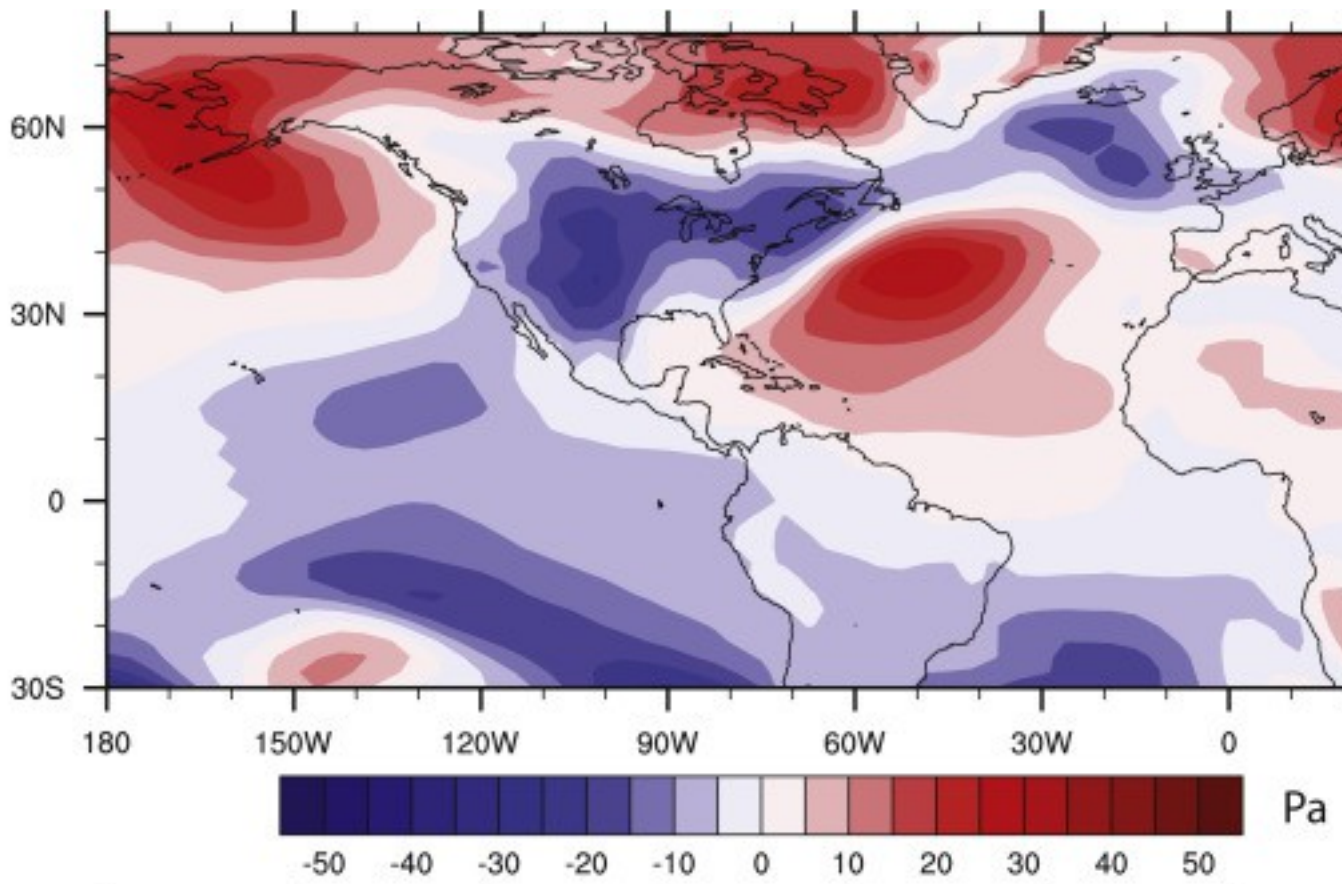
1. [Download high-res image \(937KB\)](#)
2. [Download full-size image](#)

Fig. 8. Composite plot of low-level humidity and 850 mb winds in m/s associated with the multidecadal dry periods highlighted in gray bars in Fig. 6. For HadCM3, surface humidity fields were used because atmospheric humidity fields were unavailable.

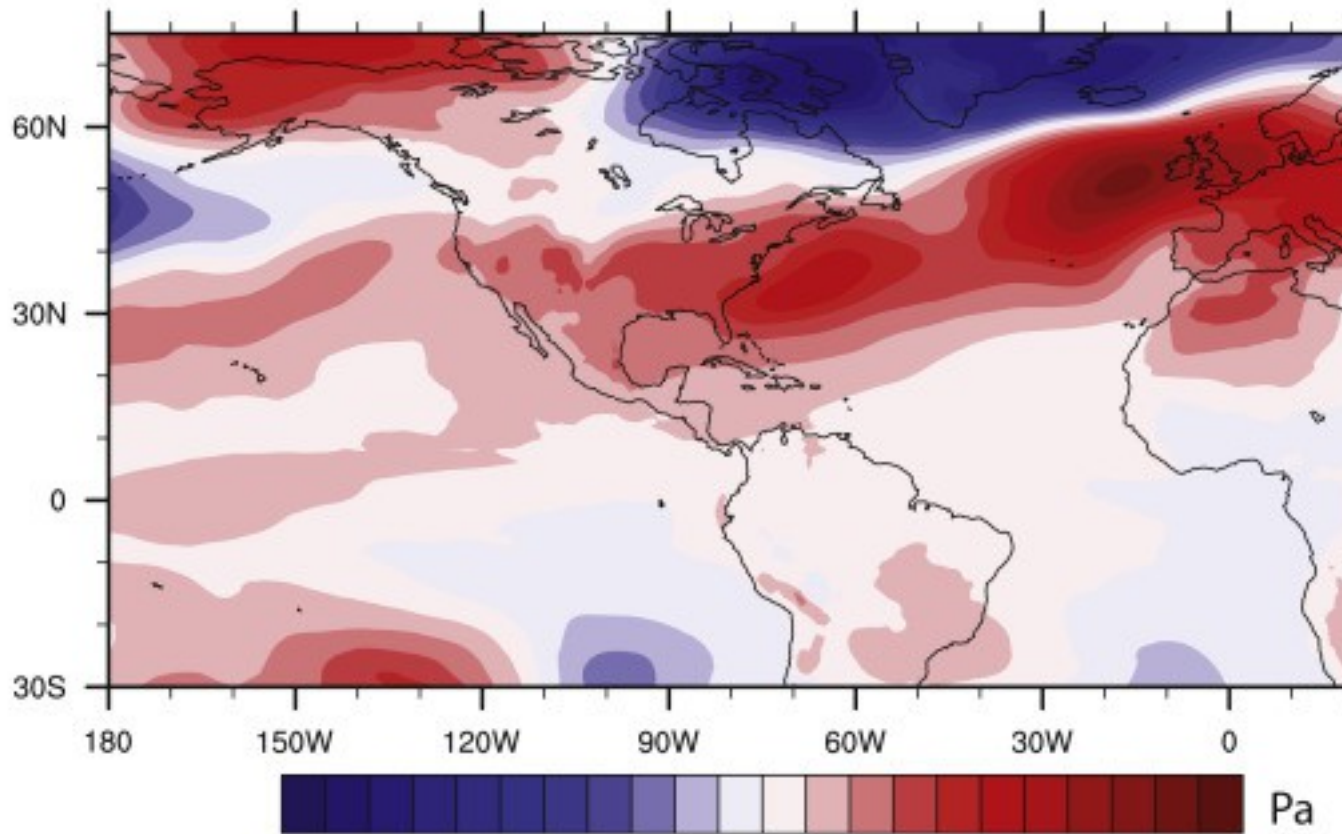
Absolute values of humidity and wind vectors are different for each model, to account for the different mean [climatology](#) and variability simulated by each model. Results reveal that the fundamental dynamics associated with droughts are similar in both CCSM4 and HadCM3: cooling in the north Atlantic reduces evaporation and boundary layer moisture over southern central America. In tandem, stronger easterly winds increase moisture divergence in southern central America while increasing moisture transport to northern Mexico or the eastern Pacific. These winds likely also further contribute to cooling as a result of the wind-evaporation-SST feedback ([Xie and Carton, 2004](#)). This overall pattern explains the dipole pattern seen in EOF1 of both models, and we also note the similarity of this pattern to the dynamics associated with the negative phase of the AMO and the positive phase of the NAO (see section [3.2](#)).

To diagnose the mechanisms behind local changes over Mesoamerica, we plot composites of [sea level pressure](#) (SLP) associated with the droughts in [Fig. 6](#). SLP Composites show that both models associate central American drying with higher SLP over the western North Atlantic, suggesting an increase in the strength of the North Atlantic Subtropical High, or NASH ([Fig. 9](#)). Differences in the SLP composites between the model simulations suggests that there are multiple drivers of Atlantic SLP changes. In HadCM3, we note a wave-like pattern from the Northern Pacific to the Atlantic sector that may be related to tropical Pacific convection, which is absent in CCSM4. HadCM3 does not show evidence of a traditional NAO-like mode, as there is anomalously high pressure over [polar regions](#) ([Fig. 9](#)). In contrast, CCSM4 contains a positive NAO-like dipole in SLP between the high latitudes and low latitudes in the north Atlantic, extending into Eurasia and North Africa. This pattern is reminiscent of SLP anomalies associated with the [Northern Annular Mode](#) ([Thompson et al., 2003](#)). It also echoes results from model experiments that cool the North Atlantic, resulting in the [advection](#) of cool, dry air downstream into Eurasia, decreasing temperatures and increasing SLP ([Liu and Chiang, 2012](#)).

HadCM3



CCSM4



1. [Download high-res image \(944KB\)](#)
2. [Download full-size image](#)

Fig. 9. Composite plot of SLP associated with the multidecadal dry periods (see [Fig. 6](#)). Note scale changes between both models' SLP plots.

4. Summary and discussion

4.1. Timing of past Mesoamerican droughts

A suite of proxy records from across Mesoamerica provide evidence of extended dry intervals over the last two millennia. Our results suggest a robust interval of drying between 800 and 1050 CE, as recorded by several lacustrine, marine, and [speleothem](#) records. This interval appears to extend over large regions of southern central America. The idea of a coherent interval of drought across Mesoamerica has been explored in other sources (see [Haug et al., 2003](#), [Douglas et al., 2016b](#), and [Lane et al. \(2014\)](#)), although this paper is unique in its attempt to systematically incorporate estimates of age uncertainty in proxy records to pinpoint this past dry interval. Most sites that show drying in this interval are in the Gulf of Mexico or southern central America.

An interesting feature of the proxy records shown in [Fig. 2](#) is that not all sites show exactly the same interval of drying: some records feature several dry intervals between 800 and 1050 CE, whereas others record a continuous dry interval. This could reflect unique features of each proxy record and proxy system. Sampling resolution can influence the timescale of climate events resolved in a proxy record; more finely sampled records may capture higher frequency climate variability than those sampled at a coarse resolution. In addition, the proxy system itself may act as a filter, helping to amplify or add low-frequency variability to the [climate signal](#): for [lake basins](#), basin size, morphology, and [vegetation cover](#) can all influence the time it takes for a lake to respond to a given [climate forcing](#), as well as the magnitude of the system's response. Similarly, different [cave systems](#) may have different residence times of groundwater in the epikarst system, introducing different levels of 'smoothing' the climate signal recorded by speleothems ([Douglas et al., 2016a](#)). This suggests that even interannual or multidecadal droughts in the climate system might ultimately register as centennial-scale dry conditions in individual proxy records. Several authors have noted that proxy records from Mesoamerica contain millennial scale variability that may not be recorded in model simulations ([Douglas et al., 2016b](#); for example, see [Fensterer et al., 2012](#)). Systematic analysis of this low-frequency climatic variability is beyond the scope of the current paper, especially given that the control simulations we analyze are only 1200–

1300 years in length. Longer control simulations, or detailed analysis of proxy systems, could begin to elucidate the causes of this millennial scale variability.

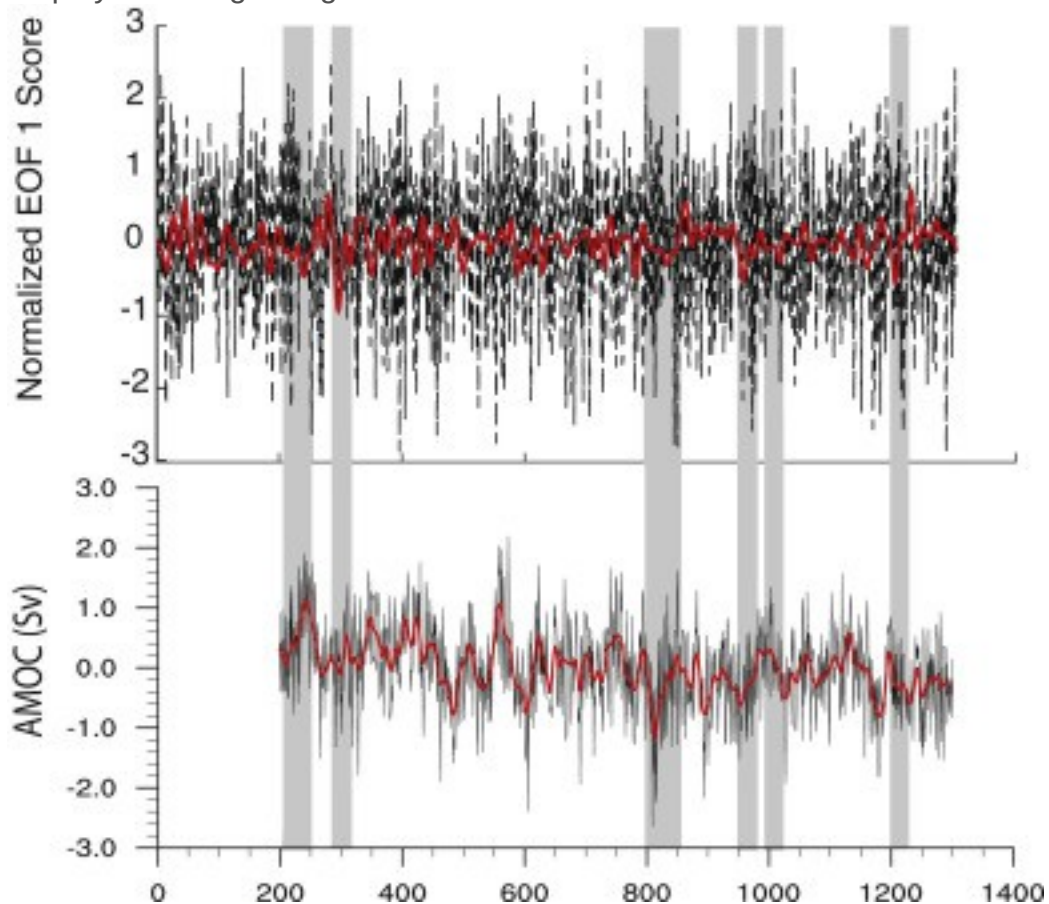
Process-based models of individual lake or cave systems can help identify the type of climate forcing recorded in paleoclimatic records. This modeling work is beyond the scope of the present study, but previous efforts at these proxy forward models has revealed interesting results. [Lake level](#) models implemented by [Medina-Elizalde and Rohling \(2012\)](#) suggest that a 25–40% reduction in annual rainfall is necessary to produce the observed proxy excursions observed during the early MCA in the Punta Laguna and Chichancanab records. Further work with forward models can pinpoint the magnitude and duration of the climatic perturbations required to produce the observed late [Holocene](#) proxy record across Mesoamerica.

4.2. Atlantic role in Mesoamerican drought

Our analysis of instrumental data and two [GCMs](#) supports a connection between Mesoamerican droughts and North Atlantic climate variability. Exploratory correlations between the AMO and NAO and Mesoamerican rainfall shows a dipole pattern, where southern central America get drier and northern Mexico gets wetter as tropical Atlantic [SSTs](#) warm ([Fig. 4](#)). This pattern is remarkably similar to the dipole pattern observed in EOF1 of both HadCM3 and CCSM4 control simulations, which is ultimately linked to changes in [boundary layer](#) moisture over Mesoamerica ([Fig. 8](#)). This pattern is the dominant EOF of both control simulations, and regression of PC1 onto rainfall data suggests that each models' PC is associated with significant changes in annual rainfall in southern central America ([Fig. 5](#), [Fig. 6](#)). Composite plots of SLP and SST in both models show strong, uniformly negative SST anomalies across the North Atlantic and higher pressure in the western North Atlantic associated with dry periods defined by EOF1 ([Fig. 7](#), [Fig. 9](#)).

SST anomalies may be linked to, but not entirely driven by, changes in the Atlantic Meridional Overturning Circulation, or AMOC. [Knight et al. \(2005\)](#) found that AMOC variations in an unforced control simulation of HadCM3 were linked with AMO-like SST changes over the North Atlantic. AMOC variability in HadCM3 has been linked in turn to the NAO and [ENSO](#) ([Vellinga and Wu, 2004](#)). Similarly, in CCSM4 previous research has shown that AMOC variability drives changes in North Atlantic SSTs, although variability in other climatic modes, like the NAO, or external forcing may drive AMOC variations ([Danabasoglu et al., 2012](#), [Cheng et al., 2013](#)). To explore this link, we plotted the AMOC index and compared it to the time periods of extended drought in CCSM4, defined as the annual mean maximum of the zonal mean meridional overturning

streamfunction at 30° N ([Cheng et al., 2013](#)). We were unable to perform this analysis for HadCM3, as the meridional overturning streamfunction was unavailable for the HadCM3 control simulation used for the other analyses in this paper. In [Fig. 10](#), we see that periods of extended drought are related to decreases in AMOC strength, but that this relationship is non-linear, with larger AMOC decreases not necessarily corresponding to stronger drying over Mesoamerica. In addition, not all decreases in the AMOC are related to Mesoamerican dry intervals. This suggests that other factors may be play in driving droughts.



1. [Download high-res image \(524KB\)](#)
2. [Download full-size image](#)

Fig. 10. Comparison of the timing of the multidecadal dry periods in [Fig. 6](#) to the AMOC index in the same model simulation. We exclude the first 200 years of the AMOC index, as the AMOC is artificially high at the beginning of the run.

One robust feature of drought in both model simulations is the concentration of high pressure over the western North Atlantic ([Fig. 9](#)). The similarity of this feature reinforces the idea that strengthened [trade winds](#) over the Caribbean play a major role in Mesoamerican dry intervals by cooling SSTs and increasing moisture divergence.

However, the dissimilarity of other features of each models' composite plots suggests that there are potentially many ways to drive SLP changes in the western North Atlantic. Neither model's SST composites look like an SST tripole associated with the NAO, although the SLP pattern in CCSM4 could suggest a more positive NAO-like feature ([Deser et al., 2010](#)). Neither model agrees on the pattern of overall SLP pattern: HadCM3 shows a PNA-like pattern, whereas CCSM4 shows an overall decrease in SLP in the mid-latitudes, especially over the Atlantic Basin ([Fig. 9](#)). This reinforces the idea that a variety of mechanisms can strengthen the NASH and SLP in the western North Atlantic, which could include remote tropical convection ([Rodwell and Hoskins, 2001](#)). Despite differences in both simulations, both CCSM4 and HadCM3 implicate Atlantic variability in low-frequency Mesoamerican drought. Both simulations feature decreases in North Atlantic SSTs and an intensification of the NASH. This change in the [ocean-atmosphere system](#) results in reduced boundary layer moisture and stronger easterly winds, causing drying over southern central America ([Fig. 8](#)). It is unclear what processes drive NASH variability in both models. Recent observational evidence suggests that atmospheric variability and ocean-atmosphere heat transfers may play a role in driving Atlantic multidecadal variability ([Bellomo et al., 2016](#), [Drews and Greatbatch, 2016](#)).

Our work coheres with several previous studies that have linked past droughts in Mesoamerica to changes in [climatic processes](#) in the North Atlantic. [Douglas et al. \(2015\)](#) mentions that the gradient of SST between the Atlantic and Pacific basins may be linked to changes in Mesoamerican hydroclimate on paleoclimatic timescales, and our work illustrates the dynamics underlying this link. [Lachniet et al. \(2017\)](#) similarly argue that synergistic processes in the Pacific and Atlantic basins may drive Mesoamerican drought, and explicitly link drought to past changes in the [North Atlantic Oscillation](#) (NAO) and ENSO. This result is further supported by the correlation between tree ring-based reconstructions of June PDSI from northern Mexico ([Stahle et al., 2012](#)). While neither [Lachniet et al. \(2017\)](#) nor [Stahle et al. \(2012\)](#) found a significant correlation between the [Atlantic Multidecadal Oscillation](#) (AMO) and their proxy records, [Stahle et al. \(2012\)](#) argue that past multidecadal intervals of drought may be more tightly coupled to changes in North Atlantic SST anomalies.

While several authors have linked changes in past Mesoamerican drought in part to changes in ENSO, especially during the late Holocene ([Lane et al., 2014](#), [Lachniet et al., 2017](#), [Wahl et al., 2014](#)), our results are equivocal about the role of ENSO. We observe a slight warming in the eastern Pacific in both drought composites, these changes are not a typical [El Niño](#) -like pattern, and are slightly south of

the [equator](#) ([Fig. 7](#)) rather than on the equator. The SLP patterns in HadCM3 suggest a wave-like pattern reminiscent of the PNA pattern that is often associated with ENSO, but this pattern is absent in the CCSM4 ([Fig. 9](#)). Rather, the common feature of both simulations are focused in the North Atlantic, suggesting that in both models, processes in the Atlantic are the dominant drivers of long-term drought.

4.3. Link between Mesoamerican rainfall variability and the ITCZ

Previous researchers have interpreted Mesoamerican drought as indicative of shifts in the mean position of the Atlantic [ITCZ](#), arguing that a southward shift in its mean position resulting in drying over Mesoamerica. In the case of the Cariaco Basin sediment flux record, [Haug et al. \(2003\)](#) have suggested that the record directly reflects mean ITCZ position. How might changes in the ITCZ be linked to the mechanism in this paper? We argue that both ITCZ position and moisture availability over Mesoamerica are linked to the interhemispheric gradient of SSTs, but via different mechanisms. While rainfall over Mesoamerica may not be linked directly to the ITCZ, it is sensitive to the same processes that govern the movement of the ITCZ. In fact, regression of our PC1 timeseries onto rainfall over the Atlantic Basin suggests a strong relationship with the position of the Atlantic ITCZ, with a more northerly(southerly) ITCZ position associated with a wetter(drier) Mesoamerica ([Figure A.14](#)).

Observational data suggests that tropical SSTs and the mean position of the ITCZ are tightly coupled. Anomalous cooling of one hemisphere results in an ITCZ shift towards the warmer hemisphere, because the ITCZ compensates for changes in cross-equatorial oceanic energy transport by transporting energy to the warmer hemisphere ([Schneider et al., 2014a](#), [Chiang and Friedman, 2012](#), [Xie and Carton, 2004](#)). A southward shift in the ITCZ can reinforce cooling in the northern hemisphere by inducing low [cloud cover](#) and stronger easterly winds that cool tropical SSTs ([Xie and Carton, 2004](#)). Even modest cooling of tropical North Atlantic SSTs can induce drying in Mesoamerica by reducing boundary layer moisture and enhancing moisture divergence ([Knight et al., 2006](#), [Xie and Carton, 2004](#)). This suggests that Mesoamerican rainfall is *linked* to shifts in the ITCZ, although the dynamical processes directly responsible for rainfall variability over Mesoamerica are separate. We next consider what mechanisms of internal climate variability or external forcing could have driven the observed dry intervals.

4.4. External forcing and other drivers of drought

Previous research has implicated both external forcing and internal climate variability in driving Mesoamerican drought. [Hodell et al. \(2001\)](#) attributed late Holocene centennial-scale changes in hydroclimate on the Yucatan Peninsula to changes in [solar activity](#). This explanation is however, inadequate for several reasons: for the time period of coherent drying between 800 and 1050 CE identified in this paper, changes in solar output, and indeed the total change in external climate forcing, is quite small in existing reconstructions ([Vieira et al., 2011](#), [Schmidt et al., 2012](#)). Even if external forcing plays a role, we emphasize that it must be communicated to the climate system via changes in the coupled atmosphere-ocean system, and is therefore most likely to manifest as a change in a known mode of climate variability, or some identifiable dynamical change in the climate system.

A recently published volcanic forcing dataset by [Sigl et al. \(2015\)](#) identifies significant volcanic eruptions in the past 2500 years, and reveals that the period between 800 and 1100 CE may be characterized by increased volcanic activity in the Northern Hemisphere as compared to the [Southern Hemisphere](#). If this is the case, we hypothesize that it could create an anomalous inter-hemispheric temperature gradient that could trigger an ITCZ shift, cooling in the tropical North Atlantic, and creating the drought pattern associate with both models' EOF1. Further study, however, is necessary to formally investigate this hypothesis.

In addition to large-scale dynamical drivers of hydroclimate, two modeling studies suggest that anthropogenic [deforestation](#) at the hands of the Maya and other pre-Columbian peoples may have amplified drought in the Maya lowlands ([Oglesby et al., 2010](#), [Cook et al., 2012](#)). Elucidating the importance of land surface changes in [paleoclimate](#) requires detailed, accurate reconstruction of population density and land use. This local mechanism could likely have acted in concert with large-scale dynamical changes in the North Atlantic to amplify local droughts.

4.5. Proxy evidence for ocean-atmosphere changes at 800–1050 CE

In this section, we examine evidence for changes in SSTs and other regions' hydroclimate that may provide clues about the causes of changes in Mesoamerican climate between 800 and 1050 CE. Identifying coherent spatiotemporal changes in ocean data is not straightforward. First, many paleoceanographic records are also dated using radiocarbon, introducing significant uncertainty into estimates of event timing. Error in the reservoir effect alone can introduce centennial-scale uncertainties into age models. Second, the uneven coverage of records makes it difficult to identify

spatially coherent changes. Low sampling resolution in some records can also hinder researchers' ability to pinpoint intervals of change.

Despite these uncertainties, oceanic records do offer some evidence for changes between 800 and 1050 CE in the North Atlantic and strongly teleconnected regions. An SST record from the Cariaco Basin shows an interval of cool [surface temperatures](#) and warming subsurface temperatures between 600 and 900 CE ([Figure A.15](#)). This could reflect a slowdown in the AMOC, or indicate stronger easterly winds that drive stronger tropical [upwelling](#) ([Wurtzel et al., 2013](#)). These easterly winds could be driven by a stronger subtropical high or a southward shifted ITCZ. Records from the northern Gulf of Mexico show modern SSTs at 800 CE, although the interval between 700 and 1100 CE is punctuated by two intervals of reduced SSTs between 750 and 900 CE and after 1000 CE ([Richey et al., 2007](#)) ([Figure A.15](#)). A record from north of Iceland also shows two periods of SST decline between 800 and 1050 CE ([Moffa-Sánchez et al., 2014](#)). Reconstructions of [ocean dynamics](#) associated with the AMOC generally show little change, although a record just north of Iceland suggests a depression in Atlantic Water incursion between 900 and 1100 CE ([Lund et al., 2006](#), [Spielhagen et al., 2011](#), [Wanamaker et al., 2012](#)). Oceanic reconstructions are therefore equivocal about north Atlantic conditions between 800 and 1050 CE, especially given the sparse coverage of available records.

Few NAO reconstructions extend back to 800 CE, but several reconstructions suggest positive conditions between 800 and 1200 CE, which would be associated with a stronger NASH ([Faust et al., 2016](#), [Baker et al., 2015](#), [Wassenburg et al., 2013](#)). A stronger NASH would drive reduced boundary layer moisture over southern central America, consistent with the mechanism summarized in Section [4.2](#). A link between the NASH and tropical north Atlantic drying is hypothesized by [Lechleitner et al. \(2017\)](#), although these authors argue that a positive NAO and stronger NASH correlates with moister conditions on the Yucatan Peninsula, at odds with the instrumental correlations and model physics that we present here. Instead, our work suggests that a positive NAO is consistent with drought in Mesoamerica.

A record of terrestrial hydroclimate from western Africa offers some support for dynamical changes in the North Atlantic region in the time period of interest ([Figure A.15](#)). Observational studies have established a link between north Atlantic cooling and weakening of summer rainfall in west Africa ([Liu and Chiang, 2012](#)). A lake level reconstruction from annually-laminated sediments at lake Bosumtwi in Ghana does in fact show evidence of dry conditions between approximately 900-1000 CE,

although individual proxies place this low-stand at slightly different time intervals ([Shanahan et al., 2009](#)). This drying is at the same time as we observe anomalous dry conditions across Mesoamerica, lending support to the idea that a change in the North Atlantic might have driven drying in both these teleconnected regions.

While we only find limited evidence for a linkage between multidecadal drought and ENSO in our GCM experiments, the instrumental record suggests that ENSO plays a strong role in the high-frequency, interannual variability of Central American climate, with warming in the eastern equatorial Pacific driving drying. Available proxy evidence does not support warming in the eastern equatorial Pacific between 800 and 1050 CE: several ENSO reconstructions lack the dating precision to pinpoint changes between 800 and 1050 CE ([Moy et al., 2002](#), [Conroy et al., 2008](#)). While one record suggests warmth in the EEP between 900 and 1150 CE, this radiocarbon-dated record is time-uncertain ([Rustic et al., 2015](#)), and a composite coral record suggests anomalously cool EEP conditions ([Cobb et al., 2003](#)). A new geochemical record from the Galapagos suggests dry conditions between 800 and 1100 CE, which could be indicative of [La Niña](#) like conditions or a northward shifted ITCZ ([Atwood and Sachs, 2014](#)). This evidence is at odds with the idea that warm ENSO events drove Mesoamerican drought between 800 and 1050 CE.

5. Conclusions and future directions

A variety of proxy records from Mesoamerica show evidence of severe drying towards the end of the first millennium CE. These droughts have been implicated in significant pre-Columbian social disruptions, and a variety of mechanisms have been proposed to explain these droughts, including shifts in the Atlantic [ITCZ](#), [ENSO](#), and changes in local [deforestation](#). Using Bayesian age modeling methods and a synthesis of available proxy records, we present evidence that there is robust evidence of drying across proxy records from 800 to 1050 CE, prior to and during the very early part of the Medieval Climate Anomaly (MCA).

Several lines of evidence lead us to suggest that Atlantic variability may be implicated in past Mesoamerican droughts, especially the dry interval between 800 and 1050 CE. First, the correlation between the AMO and NAO and Mesoamerican rainfall in the instrumental record shows that the cooling of tropical North Atlantic [SSTs](#) dries southern central America and increases rainfall in northern Mexico. This dipole is also the dominant mode of variability, or EOF, in control simulations of HadCM3 and CCSM4 and extended dry intervals recorded by this mode result in up to 20–30% of rainfall reductions in southern central America. Drying in both models is driven by basin-wide

cooling in the North Atlantic, intensification of the NASH, and atmospheric drying over southern central America. In the models this is also associated with an enhanced interhemispheric gradient of temperature and a southward shifted ITCZ. While SST evidence is sparse, there is some evidence for stronger easterlies near northern South America and SST variability in the period of interest. Furthermore, hydroclimate records from west Africa also support the idea of tropical North Atlantic cooling in this interval. Future research can test the link between Atlantic variability and Mesoamerican climate using explicit model simulations that prescribe Atlantic cooling. This analysis using a suite of [GCMs](#) could help establish the sensitivity of regional rainfall to Atlantic variability. Forward models of different proxy systems can also pinpoint whether an observed or modeled [climate change](#) is sufficient to produce the magnitude and timing of climate changes observed in the proxy record. Additional high-resolution, well-dated proxy records from across Mesoamerica and from the North Atlantic can also help clarify the pattern of regional hydroclimate change between 800 and 1050 CE and test its relationship to Atlantic variability.

Acknowledgments

This material is based upon work supported by the National Science Foundation Graduate Research Fellowship under Grant No. [DGE 1106400](#). Additional funding comes from NSF DDRIG No. [BCS-13333370](#), and a U.C. Museum of Paleontology Graduate Research Award (2013–2014, 2014–2015) and NOAA grants [NA16OAR4310171](#) to J.C.H. Chiang and [NA16OAR4310169](#) to W. Cheng. We thank Jeff Knight for help with HadCM3 output. We thank current and past members of the U.C. Berkeley Climate ‘Supergroup,’ David Wahl, Roger Byrne, Ben Cook, and others for helpful suggestions and discussions.

Appendix B. Supplementary data

The following is the supplementary data related to this article:

[Download Acrobat PDF file \(2MB\)Help with pdf files](#)

Online data.

References

[Akers et al., 2016](#)

P.D. Akers, G.A. Brook, L.B. Railsback, F. Liang, G. Iannone, J.W. Webster, P.P. Reeder, H. Cheng, R.L. Edwards **An extended and higher-resolution record of climate and land use from stalagmite mc01 from macal chasm, Belize, revealing connections between major dry events, overall climate variability, and maya sociopolitical changes**

Palaeogeogr. Palaeoclimatol. Palaeoecol., 459 (2016), pp. 268-288

[ArticleDownload PDFView Record in Scopus](#)

[Atwood and Sachs, 2014](#)

A.R. Atwood, J.P. Sachs **Separating itcz-and enso-related rainfall changes in the galápagos over the last 3 kyr using d/h ratios of multiple lipid biomarkers**

Earth Planet. Sci. Lett., 404 (2014), pp. 408-419

[ArticleDownload PDFView Record in Scopus](#)

[Baker et al., 2015](#)

A. Baker, J.C. Hellstrom, B.F. Kelly, G. Mariethoz, V.Trouet **A composite annual-resolution stalagmite record of north atlantic climate over the last three millennia**

Sci. Rep., 5 (2015), p. 10307

[Bellomo et al., 2016](#)

K. Bellomo, A.C. Clement, L.N. Murphy, L.M. Polvani, M.A. Cane **New observational evidence for a positive cloud feedback that amplifies the atlantic multidecadal oscillation**

Geophys. Res. Lett., 43 (18) (2016), pp. 9852-9859

[CrossRefView Record in Scopus](#)

[Bhattacharya et al., 2015](#)

T. Bhattacharya, R. Byrne, H. Böhnelt, K. Wogau, U. Kienel, B.L. Ingram, S. Zimmerman **Cultural implications of late holocene climate change in the cuenca oriental, mexico**

Proc. Natl. Acad. Sci., 112 (6) (2015), pp. 1693-1698

[CrossRefView Record in Scopus](#)

[Bhattacharya and Chiang, 2014](#)

T. Bhattacharya, J.C. Chiang **Spatial variability and mechanisms underlying el niño-induced droughts in mexico**

Clim. Dyn., 43 (12) (2014), pp. 3309-3326

[CrossRefView Record in Scopus](#)

[Blaauw et al., 2011](#)

M. Blaauw, J.A. Christen, *et al.* **Flexible paleoclimate age-depth models using an autoregressive gamma process**

Bayesian Anal., 6 (3) (2011), pp. 457-474

[CrossRefView Record in Scopus](#)

[Cheng et al., 2013](#)

W. Cheng, J.C. Chiang, D. Zhang **Atlantic meridional overturning circulation (amoc) in cmip5 models: Rcp and historical simulations**

J. Clim., 26 (18) (2013), pp. 7187-7197

[CrossRefView Record in Scopus](#)

[Chiang and Friedman, 2012](#)

J.C. Chiang, A.R. Friedman **Extratropical cooling, interhemispheric thermal gradients, and tropical climate change**

Annu. Rev. Earth Planet. Sci., 40 (1) (2012), p. 383

[CrossRefView Record in Scopus](#)

[Chiang and Sobel, 2002](#)

J.C. Chiang, A.H. Sobel **Tropical tropospheric temperature variations caused by enso and their influence on the remote tropical climate***

J. Clim., 15 (18) (2002), pp. 2616-2631

[CrossRefView Record in Scopus](#)

[Cobb et al., 2003](#)

K.M. Cobb, C.D. Charles, H. Cheng, R.L. Edwards **El nino/southern oscillation and tropical pacific climate during the last millennium**

Nature, 424 (6946) (2003), pp. 271-276

[CrossRefView Record in Scopus](#)

[Conroy et al.,](#)

[2008](#)

J.L. Conroy, J.T. Overpeck, J.E. Cole, T.M. Shanahan, M. Steinitz-Kannan **Holocene changes in eastern tropical pacific climate inferred from a galápagos lake sediment record**

Quat. Sci. Rev., 27 (11) (2008), pp. 1166-1180

[ArticleDownload PDFView Record in Scopus](#)

[Cook](#)

[et al.,](#)

[2012](#)

B. Cook, K. Anchukaitis, J. Kaplan, M. Puma, M. Kelley, D. Gueyffier **Pre-columbian deforestation as an amplifier of drought in mesoamerica**

Geophys. Res. Lett., 39 (16) (2012)

[C](#)
[u](#)
[r](#)
[t](#)
[i](#)
[s](#)
[-](#)
[e](#)
[t](#)
[-](#)
[a](#)
[l](#)
[-](#)
[-](#)

[1](#)
[9](#)
[9](#)
[6](#)

J.H. Curtis, D.A. Hodell, M. Brenner **Climate variability on the yucatan peninsula (mexico) during the past 3500 years, and implications for maya cultural evolution**

Quat. Res., 46 (1) (1996), pp. 37-47

[ArticleDownload PDF](#) [CrossRefView Record in Scopus](#)

[Danaba
soglu
et al.,
2012](#)

G. Danabasoglu, S.G. Yeager, Y.-O. Kwon, J.J. Tribbia, A.S. Phillips, J.W. Hurrell **Variability of the atlantic meridional overturning circulation in ccsm4**

J. Clim., 25 (15) (2012), pp. 5153-5172

[CrossRefView Record in Scopus](#)

[Deser et al.,
2010](#)

C. Deser, M.A. Alexander, S.-P. Xie, A.S. Phillips **Sea surface temperature variability: patterns and mechanisms**

Annu. Rev. Mar. Sci., 2 (2010), pp. 115-143

[CrossRefView Record in Scopus](#)

[Douglas et al., 2016](#)

P.M. Douglas, M. Brenner, J.H. Curtis **Methods and future directions for paleoclimatology in the maya lowlands**

Glob. Planet. Change, 138 (2016), pp. 3-24

[ArticleDownload PDF](#) [View Record in Scopus](#)

[Douglas et al., 2016](#)

P.M. Douglas, A.A. Demarest, M. Brenner, M.A. Canuto **Impacts of climate change on the collapse of lowland maya civilization**

Annu. Rev. Earth Planet. Sci., 44 (2016), pp. 613-645

[CrossRefView Record in Scopus](#)

[Douglas et al., 2016](#)

P.M. Douglas, M. Pagani, M.A. Canuto, M. Brenner, D.A. Hodell, T.I. Eglinton, J.H. Curtis **Drought , agricultural adaptation, and sociopolitical collapse in the maya lowlands**

Proc. Natl. Acad. Sci., 112 (18) (2015), pp. 5607-5612

[CrossRefView Record in Scopus](#)

[Drews and Gra...](#)

A. Drews, R.J. Greatbatch **Atlantic multidecadal variability in a model with an improved north atlantic current**

Geophys. Res. Lett., 43 (15) (2016), pp. 8199-8206

[CrossRefView Record in Scopus](#)

[Enfield et al., 200](#)

D.B. Enfield, A.M. Mestas-Nuñez, P.J. Trimble **The atlantic multidecadal oscillation and its relation to rainfall and river flows in the continental us**

Geophys. Res. Lett., 28 (10) (2001), pp. 2077-2080

[CrossRefView Record in Scopus](#)

[Faust et al., 201](#)

J.C. Faust, K. Fabian, G. Milzer, J. Giraudeau, J. Knies **Norwegian fjord sediments reveal nao related winter temperature and precipitation changes of the past 2800 years**

Earth Planet. Sci. Lett., 435 (2016), pp. 84-93

[ArticleDownload PDFView Record in Scopus](#)

[Fensterer et al.,](#)

C. Fensterer, D. Scholz, D. Hoffmann, C. Spötl, J.M.Pajón, A. Mangini **Cuban Stalagmite Suggests Relationship between Caribbean Precipitation and the Atlantic Multidecadal Oscillation during the Past 1.3 Ka**

The Holocene (2012)

0959683612449759

[Gent et al., 2011](#)

P.R. Gent, G. Danabasoglu, L.J. Donner, M.M. Holland, E.C. Hunke, S.R. Jayne, D.M. Lawrence, R.B. Neale, P.J. Rasch, M. Vertenstein, *et al.* **The community climate system model version 4**

J. Clim., 24 (19) (2011), pp. 4973-4991

[CrossRefView Record in Scopus](#)

[Giannini et al., 2](#)

A. Giannini, M.A. Cane, Y. Kushnir **Interdecadal changes in the enso teleconnection to the caribbean region and the north atlantic oscillation***

J. Clim., 14 (13) (2001), pp. 2867-2879

[CrossRefView Record in Scopus](#)

[Giannini et al., 2](#)

A. Giannini, J.C. Chiang, M.A. Cane, Y. Kushnir, R. Seager **The enso teleconnection to the tropical atlantic ocean: contributions of the remote and local ssts to rainfall variability in the tropical americas***

J. Clim., 14 (24) (2001), pp. 4530-4544

[CrossRefView Record in Scopus](#)

[Giannini et al., 2](#)

A. Giannini, Y. Kushnir, M.A. Cane **Interannual variability of caribbean rainfall, enso, and the atlantic ocean***

J. Clim., 13 (2) (2000), pp. 297-311

[CrossRefView Record in Scopus](#)

[Gordon et al., 2000](#)

C. Gordon, C. Cooper, C.A. Senior, H. Banks, J.M.Gregory, T.C. Johns, J.F. Mitchell, R.A. Wood
**the simulation of sst, sea ice extents and ocean heat transports in a version of the hadley
centre coupled model without flux adjustments**

Clim. Dyn., 16 (2–3) (2000), pp. 147-168

[CrossRefView Record in Scopus](#)

[Haug et al., 2003](#)

G.H. Haug, D. Günther, L.C. Peterson, D.M. Sigman, K.A.Hughen, B. Aeschlimann
Climate and the collapse of maya civilization

Science, 299 (5613) (2003), pp. 1731-1735

[CrossRefView Record in Scopus](#)

[Hodell et al., 2003](#)

D.A. Hodell, M. Brenner, J.H. Curtis
**Terminal classic drought in the northern maya lowlands
inferred from multiple sediment cores in lake chichancanab (mexico)**

Quat. Sci. Rev., 24 (12) (2005), pp. 1413-1427

[ArticleDownload PDFView Record in Scopus](#)

[Hodell et al., 2005](#)

D.A. Hodell, M. Brenner, J.H. Curtis, T. Guilderson
**Solar forcing of drought frequency in the
maya lowlands**

Science, 292 (5520) (2001), pp. 1367-1370

[CrossRefView Record in Scopus](#)

[Hodell et al., 2001](#)

D.A. Hodell, M. Brenner, J.H. Curtis, R. Medina-González, E.I.-C. Can, A. Albornaz-Pat, T.P. Guil
derson
Climate change on the yucatan peninsula during the little ice age

Quat. Res., 63 (2) (2005), pp. 109-121

[ArticleDownload PDFCrossRefView Record in Scopus](#)

[Hodell et al., 1999](#)

D.A. Hodell, J.H. Curtis, M. Brenner
**Possible role of climate in the collapse of classic maya
civilization**

Nature, 375 (6530) (1995), pp. 391-394

[CrossRefView Record in Scopus](#)

[Hurrell and Deser](#)

J.W. Hurrell, C. Deser
**North atlantic climate variability: the role of the north atlantic
oscillation**

J. Mar. Syst., 79 (3) (2010), pp. 231-244

[ArticleDownload PDFView Record in Scopus](#)

[Kennett et al., 2001](#)

D.J. Kennett, S.F. Breitenbach, V.V. Aquino, Y. Asmerom, J. Awe, J.U. Baldini, P. Bartlein, B.J. Culleton, C. Ebert, C. Jazwa, *et al.* **Development and disintegration of maya political systems in response to climate change**

Science, 338 (6108) (2012), pp. 788-791

[CrossRefView Record in Scopus](#)

[Knight et al., 2012](#)

J.R. Knight, R.J. Allan, C.K. Folland, M. Vellinga, M.E. Mann **A signature of persistent natural thermohaline circulation cycles in observed climate**

Geophys. Res. Lett., 32 (20) (2005)

[Knight et al., 2005](#)

J.R. Knight, C.K. Folland, A.A. Scaife **Climate impacts of the atlantic multidecadal oscillation**

Geophys. Res. Letters, 33 (17) (2006)

[Lachniet et al., 2017](#)

M.S. Lachniet, Y. Asmerom, V. Polyak, J.P. Bernal **Two millennia of mesoamerican monsoon variability driven by pacific and atlantic synergistic forcing**

Quat. Sci. Rev., 155 (2017), pp. 100-113

[ArticleDownload PDFView Record in Scopus](#)

[Lachniet et al., 2017](#)

M.S. Lachniet, J.P. Bernal, Y. Asmerom, V. Polyak, D. Piperno **A 2400 yr mesoamerican rainfall reconstruction links climate and cultural change**

Geology, 40 (3) (2012), pp. 259-262

[CrossRefView Record in Scopus](#)

[Lachniet et al., 2012](#)

M.S. Lachniet, S.J. Burns, D.R. Piperno, Y. Asmerom, V.J. Polyak, C.M. Moy, K. Christenson **A 1500-year el niño/southern oscillation and rainfall history for the isthmus of Panama from speleothem calcite**

J. Geophys. Res. Atmos., 109 (D20) (2004)

[Lane et al., 2014](#)

C.S. Lane, S.P. Horn, M.T. Kerr **Beyond the mayan lowlands: impacts of the terminal classic drought in the caribbean antilles**

Quat. Sci. Rev., 86 (2014), pp. 89-98

[ArticleDownload PDFView Record in Scopus](#)

[Lechleitner et al., 2014](#)

F.A. Lechleitner, S.F. Breitenbach, K. Rehfeld, H.E. Ridley, Y. Asmerom, K.M. Prufer, N. Marwan, B. Goswami, D.J. Kennett, V.V. Aquino, *et al.* **Tropical rainfall over the last two millennia: evidence for a low-latitude hydrologic seesaw**

Sci. Rep., 7 (2017)

[Liu and Chiang, 2017](#)

Y. Liu, J. Chiang **Coordinated abrupt weakening of the eurasian and north african monsoons in the 1960s and links to extratropical north atlantic cooling**

J. Clim., 25 (10) (2012), pp. 3532-3548

[CrossRefView Record in Scopus](#)

[Lund et al., 2006](#)

D.C. Lund, J. Lynch-Stieglitz, W.B. Curry **Gulf stream density structure and transport during the past millennium**

Nature, 444 (7119) (2006), pp. 601-604

[CrossRefView Record in Scopus](#)

[Magaña et al., 2003](#)

V.O. Magaña, J.L. Vázquez, J.L. Pérez, J.B. Pérez **Impact of el niño on precipitation in mexico**

Geofis. Internacional-Mexico-, 42 (3) (2003), pp. 313-330

[View Record in Scopus](#)

[Mann et al., 2009](#)

M.E. Mann, Z. Zhang, S. Rutherford, R.S. Bradley, M.K. Hughes, D. Shindell, C. Ammann, G. Falu vegi, F. Ni **Global signatures and dynamical origins of the little ice age and medieval climate anomaly**

Science, 326 (5957) (2009), pp. 1256-1260

[CrossRefView Record in Scopus](#)

[Mantua et al., 1997](#)

N.J. Mantua, S.R. Hare, Y. Zhang, J.M. Wallace, R.C. Francis **A pacific interdecadal climate oscillation with impacts on salmon production**

Bull. Am. Meteorological Soc., 78 (6) (1997), pp. 1069-1079

[CrossRefView Record in Scopus](#)

[Medina-Elizalde et al., 2010](#)

M. Medina-Elizalde, S.J. Burns, D.W. Lea, Y. Asmerom, L. von Gunten, V. Polyak, M. Vuille, A. Karmalkar **High resolution stalagmite climate record from the yucatán peninsula spanning the maya terminal classic period**

Earth Planet. Sci. Lett., 298 (1) (2010), pp. 255-262

[ArticleDownload PDFView Record in Scopus](#)

[Medina-Elizalde and Rohling, 2012](#)

M. Medina-Elizalde, E.J. Rohling **Collapse of classic maya civilization related to modest reduction in precipitation**

Science, 335 (6071) (2012), pp. 956-959

[CrossRefView Record in Scopus](#)

[Méndez and Magaña, 2010](#)

M. Méndez, V. Magaña **Regional aspects of prolonged meteorological droughts over mexico and central America**

J. Clim., 23 (5) (2010), pp. 1175-1188

[CrossRefView Record in Scopus](#)

[Mestas-Nuñez et al., 2007](#)

A.M. Mestas-Nuñez, D.B. Enfield, C. Zhang **Water vapor fluxes over the intra-americas sea: seasonal and interannual variability and associations with rainfall**

J. Clim., 20 (9) (2007), pp. 1910-1922

[CrossRefView Record in Scopus](#)

[Moffa-Sánchez et al., 2014](#)

P. Moffa-Sánchez, A. Born, I.R. Hall, D.J.Thornalley, S. Barker **Solar forcing of north atlantic surface temperature and salinity over the past millennium**

Nat. Geosci., 7 (4) (2014), pp. 275-278

[CrossRefView Record in Scopus](#)

[Moy et al., 2002](#)

C.M. Moy, G.O. Seltzer, D.T. Rodbell, D.M. Anderson **Variability of el niño/southern oscillation activity at millennial timescales during the holocene epoch**

Nature, 420 (6912) (2002), pp. 162-165

[CrossRefView Record in Scopus](#)

[Oglesby et al., 2010](#)

R.J. Oglesby, T.L. Sever, W. Saturno, D.J. Erickson, J.Srikishen **Collapse of the maya: could deforestation have contributed?**

J. Geophys. Res. Atmos., 115 (D12) (2010)

[Richey et al., 2007](#)

J.N. Richey, R.Z. Poore, B.P. Flower, T.M. Quinn **1400 yr multiproxy record of climate variability from the northern gulf of mexico**

Geology, 35 (5) (2007), pp. 423-426

[CrossRefView Record in Scopus](#)

[Risi et al., 2008](#)

C. Risi, S. Bony, F. Vimeux **Influence of convective processes on the isotopic composition ($\delta^{18}O$ and δD) of precipitation and water vapor in the tropics: 2. physical interpretation of the amount effect**

J. Geophys. Res. Atmos., 113 (D19) (2008)

[Rodwell and Hoskins, 2001](#)

M.J. Rodwell, B.J. Hoskins **Subtropical anticyclones and summer monsoons**

J. Clim., 14 (15) (2001), pp. 3192-3211

[CrossRefView Record in Scopus](#)

[Rosenmeier et al., 2002](#)

M.F. Rosenmeier, D.A. Hodell, M. Brenner, J.H.Curtis, T.P. Guilderson **A 4000-year lacustrine record of environmental change in the southern maya lowlands, petén, Guatemala**

Quat. Res., 57 (2) (Mar. 2002), pp. 183-190

<http://linkinghub.elsevier.com/retrieve/pii/S0033589401923051>

[ArticleDownload PDFCrossRefView Record in Scopus](#)

[Rustic et al., 2015](#)

G.T. Rustic, A. Koutavas, T.M. Marchitto, B.K. Linsley **Dynamical excitation of the tropical pacific ocean and enso variability by little ice age cooling**

Science, 350 (6267) (2015), pp. 1537-1541

[CrossRefView Record in Scopus](#)

[Schmidt et al., 2012](#)

G. Schmidt, J. Jungclaus, C. Ammann, E. Bard, P. Braconnot, T. Crowley, G. Delaygue, F. Joos, N. Krivova, R. Muscheler, *et al.* **Climate forcing reconstructions for use in pmip simulations of the last millennium (v1. 1)**

Geosci. Model Dev., 5 (2012), pp. 185-191

[CrossRefView Record in Scopus](#)

[Schneider et al., 2014a](#)

T. Schneider, T. Bischoff, G.H. Haug **Migrations and dynamics of the intertropical convergence zone**

Nature, 513 (7516) (2014), pp. 45-53

[CrossRefView Record in Scopus](#)

[Schneider et al., 2014b](#)

U. Schneider, A. Becker, P. Finger, A. Meyer-Christoffer, M. Ziese, B. Rudolf **Gpcc's new land surface precipitation climatology based on quality-controlled in situ data and its role in quantifying the global water cycle**

Theor. Appl. Climatol., 115 (1–2) (2014), pp. 15-40

<http://link.springer.com/10.1007/s00704-013-0860-x>

[CrossRefView Record in Scopus](#)

[Shanahan et al., 2009](#)

T.M. Shanahan, J.T. Overpeck, K. Anchukaitis, J.W. Beck, J.E. Cole, D.L. Dettman, J.A. Peck, C.A. Scholz, J.W. King **Atlantic forcing of persistent drought in west africa**

science, 324 (5925) (2009), pp. 377-380

[CrossRefView Record in Scopus](#)

[Sigl et al., 2015](#)

M. Sigl, M. Winstrup, J. McConnell, K. Welten, G. Plunkett, F. Ludlow, U. Büntgen, M. Caffee, N. Chellman, D. Dahl-Jensen, *et al.* **Timing and climate forcing of volcanic eruptions for the past 2,500 years**

Nature, 523 (7562) (2015), pp. 543-549

[CrossRefView Record in Scopus](#)

[Spielhagen et al., 2011](#)

R.F. Spielhagen, K. Werner, S.A. Sørensen, K. Zamelczyk, E. Kandiano, G. Budeus, K. Husum, T. M. Marchitto, M. Hald **Enhanced modern heat transfer to the arctic by warm atlantic water**

Science, 331 (6016) (2011), pp. 450-453

[CrossRefView Record in Scopus](#)

[Stahle et al., 2012](#)

D. Stahle, D. Burnette, J.V. Díaz, R. Heim, F. Fye, J.C.Paredes, R.A. Soto, M. Cleaveland **Pacific and atlantic influences on mesoamerican climate over the past millennium**

Clim. Dyn., 39 (6) (2012), pp. 1431-1446

[CrossRefView Record in Scopus](#)

[Stansell et al., 2013](#)

N.D. Stansell, B.A. Steinman, M.B. Abbott, M. Rubinov, M. Roman-Lacayo **Lacustrine stable isotope record of precipitation changes in Nicaragua during the little ice age and medieval climate anomaly**

Geology, 41 (2) (2013), pp. 151-154

[CrossRefView Record in Scopus](#)

[Thompson et al., 2003](#)

D.W. Thompson, S. Lee, M.P. Baldwin **Atmospheric processes governing the northern hemisphere annular mode/north atlantic oscillation**

N. Atl. Oscillation Clim. significance Environ. impact (2003), pp. 81-112

[CrossRefView Record in Scopus](#)

[Trenberth, 1997](#)

K.E. Trenberth **The definition of el nino**

Bull. Am. Meteorological Soc., 78 (12) (1997), p. 2771

[CrossRefView Record in Scopus](#)

[Uppala et al., 2005](#)

S.M. Uppala, P. Kållberg, A. Simmons, U. Andrae, V.

dBechtold, M. Fiorino, J. Gibson, J. Haseler, A. Hernandez, G. Kelly, *et al.* **The era-40 re-analysis**

Q. J. R. Meteorological Soc., 131 (612) (2005), pp. 2961-3012

[CrossRefView Record in Scopus](#)

[van Hengstum et al., 2016](#)

P.J. van Hengstum, J.P. Donnelly, P.L. Fall, M.R. Toomey, N.A. Albury, B. Kakuk **The intertropical convergence zone modulates intense hurricane strikes on the western north atlantic margin**

Sci. Rep., 6 (2016)

[Vellinga and Wu, 2004](#)

M. Vellinga, P. Wu **Low-latitude freshwater influence on centennial variability of the atlantic thermohaline circulation**

J. Clim., 17 (23) (2004), pp. 4498-4511

[CrossRefView Record in Scopus](#)

[Vieira et al., 2011](#)

L.E.A. Vieira, S.K. Solanki, N.A. Krivova, I. Usoskin **Evolution of the solar irradiance during the holocene**

Astronomy Astrophysics, 531 (2011), p. A6

[CrossRef](#)

[Wahl et al., 2014](#)

D. Wahl, R. Byrne, L. Anderson **An 8700 year paleoclimate reconstruction from the southern maya lowlands**

Quat. Sci. Rev., 103 (2014), pp. 19-25

[ArticleDownload PDFView Record in Scopus](#)

[Wahl et al., 2013](#)

D. Wahl, F. Estrada-Belli, L. Anderson **A 3400 year paleolimnological record of prehispanic human–environment interactions in the holmul region of the southern maya lowlands**

Palaeogeogr. Palaeoclimatol. Palaeoecol., 379 (2013), pp. 17-31

[ArticleDownload PDFView Record in Scopus](#)

[Wanamaker et al., 2012](#)

A.D. Wanamaker Jr., P.G. Butler, J.D. Scourse, J. Heinemeier, J. Eiriksson, K.L. Knudsen, C.A. Richardson **Surface changes in the north atlantic meridional overturning circulation during the last millennium**

Nat. Commun., 3 (2012), p. 899

[Wang, 2007](#)

C. Wang **Variability of the caribbean low-level jet and its relations to climate**

Clim. Dyn., 29 (4) (2007), pp. 411-422

[CrossRefView Record in Scopus](#)

[Wang et al., 2008](#)

C. Wang, S.-K. Lee, D.B. Enfield **Climate response to anomalously large and small atlantic warm pools during the summer**

J. Clim., 21 (11) (2008), pp. 2437-2450

[CrossRefView Record in Scopus](#)

[Wassenburg et al., 2013](#)

J. Wassenburg, A. Immenhauser, D. Richter, A. Niedermayr, S. Riechelmann, J. Fietzke, D. Scholz, K. Jochum, J. Fohlmeister, A. Schröder-Ritzrau, *et al.* **Moroccan speleothem and tree ring records suggest a variable positive state of the north atlantic oscillation during the medieval warm period**

Earth Planet. Sci. Lett., 375 (2013), pp. 291-302

[ArticleDownload PDFView Record in Scopus](#)

[Webster et al., 2007](#)

J.W. Webster, G.A. Brook, L.B. Railsback, H. Cheng, R.L. Edwards, C. Alexander, P.P. Reeder **Stalagmite evidence from Belize indicating significant droughts at the time of preclassic abandonment, the maya hiatus, and the classic maya collapse**

Palaeogeogr. Palaeoclimatol. Palaeoecol., 250 (1) (2007), pp. 1-17

[ArticleDownload PDFView Record in Scopus](#)

[Woodruff et al., 2008](#)

J.D. Woodruff, J.P. Donnelly, K. Emanuel, P. Lane **Assessing sedimentary records of paleohurricane activity using modeled hurricane climatology**

Geochem. Geophys. Geosystems, 9 (9) (2008)

[Wurtzel et al., 2013](#)

J.B. Wurtzel, D.E. Black, R.C. Thunell, L.C. Peterson, E.J. Tappa, S. Rahman **Mechanisms of southern caribbean sst variability over the last two millennia**

Geophys. Res. Lett., 40 (22) (2013), pp. 5954-5958

[CrossRefView Record in Scopus](#)

[Xie and Carton, 2004](#)

S.-P. Xie, J.A. Carton **Tropical atlantic variability: patterns, mechanisms, and impacts**

Earth's Clim. (2004), pp. 121-142

[View Record in Scopus](#)